Nanomechanical resonators

Transduction via electrical and optical gradient forces

Jörg P. Kotthaus

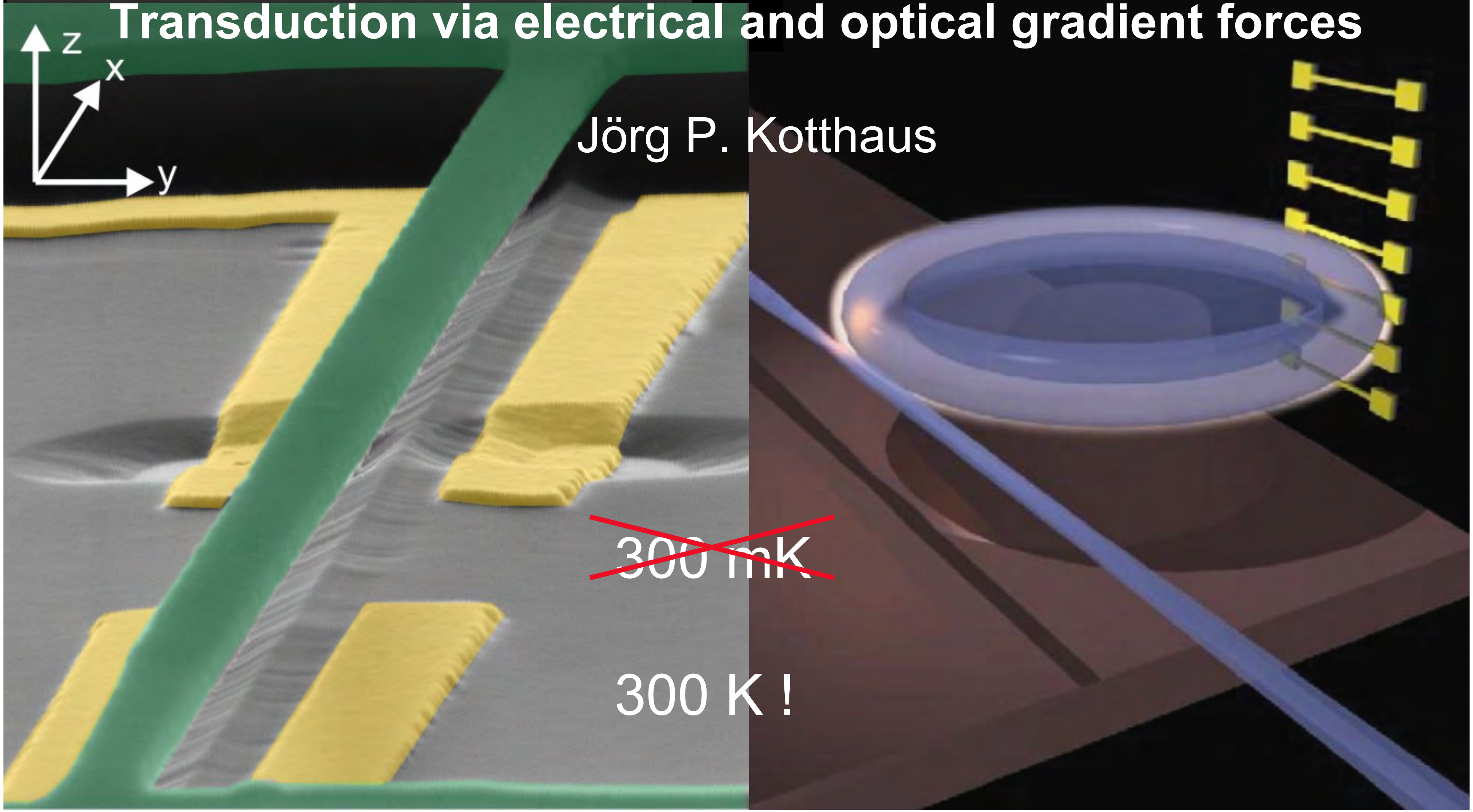

~~300 mK~~

300 K !

Why NanoElectroMechanical Systems (NEMS)? Sensing of masses, forces, displacements

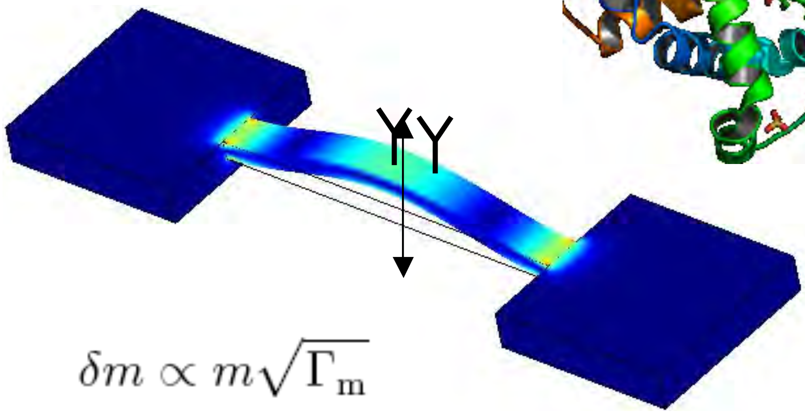

$$\delta m \propto m\sqrt{\Gamma_m}$$

$$\delta F \propto \sqrt{m\Gamma_m}$$

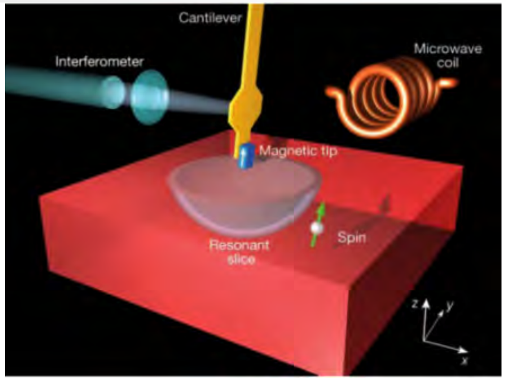

Force sensing with single spin sensitivity
D. Rugar et al., Nature, **430**, 329 (2004)

Highly scalable
here:10^4/mm^2

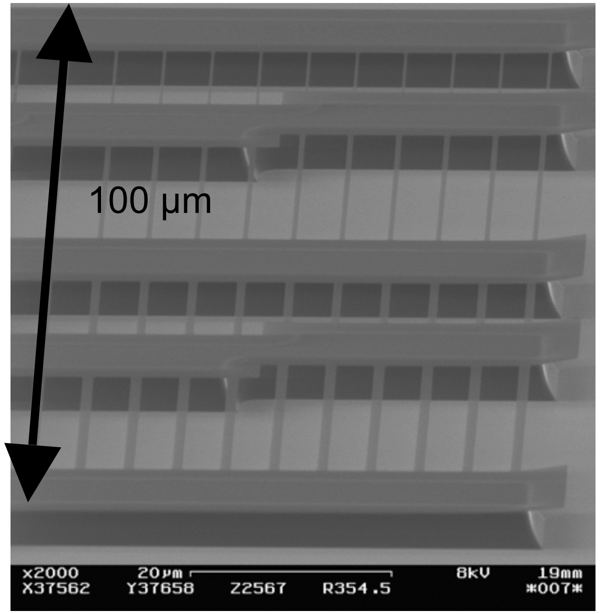

Mass detection with single atom resolution

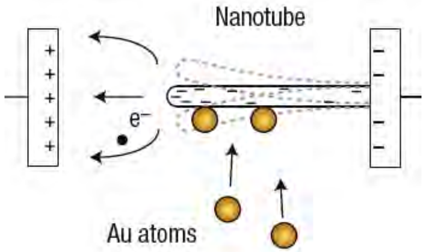

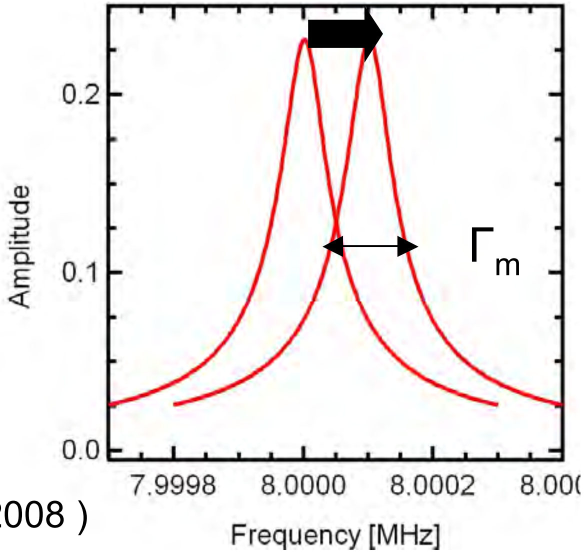

K. Jensen et al.,
Nature Nanotech **3**, 533 (2008)

Why NanoElectroMechanical Systems (NEMS)?
Some fundamental science problems

Fundamental Science

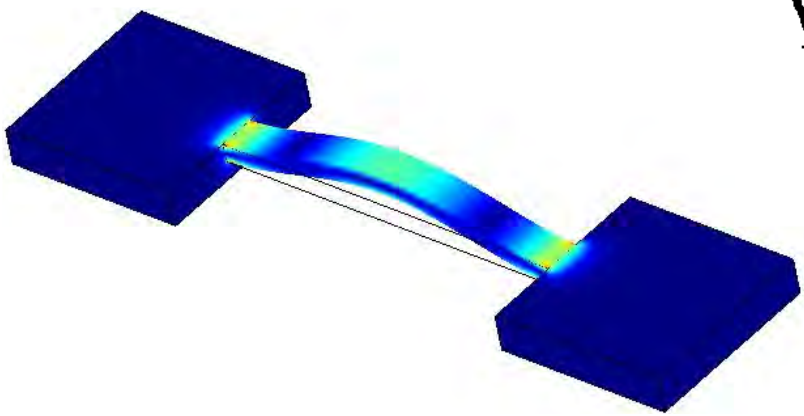

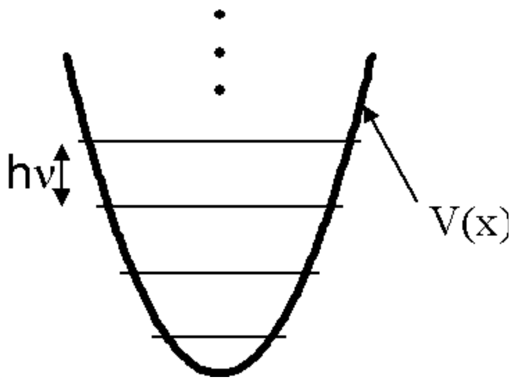

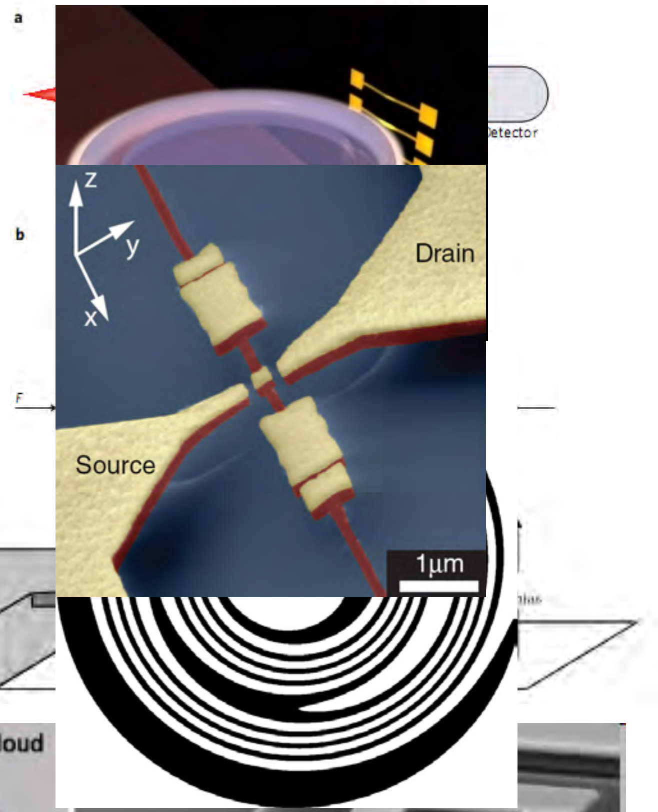

- Zero Point Motion - QNEMS
- Single Electron Shuttle
- Nonlinear Mechanics
- Cavity NanoOptoMechanics
- Hybrid Systems

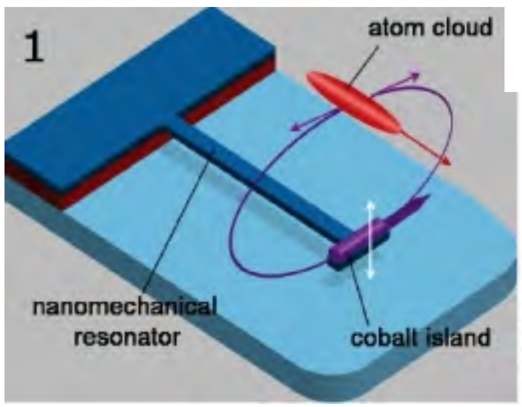

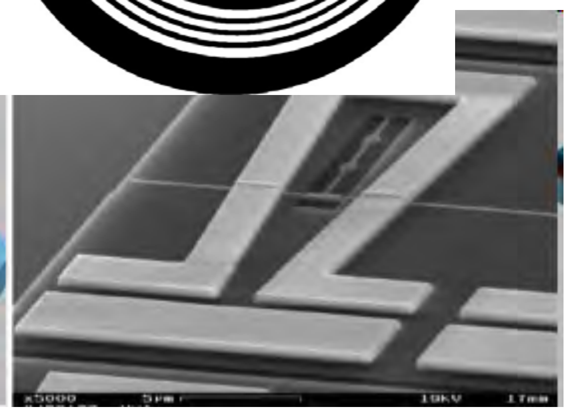

Outline

- Actuation by electrical gradient fields
- Detection on-chip interferometric and self-oscillation
- Non-linear behavior and induced switching
- Damping and mechanical quality factor
- Optical gradient field actuation and
- Quantum limited detection
- Shuttling charge with NEMS

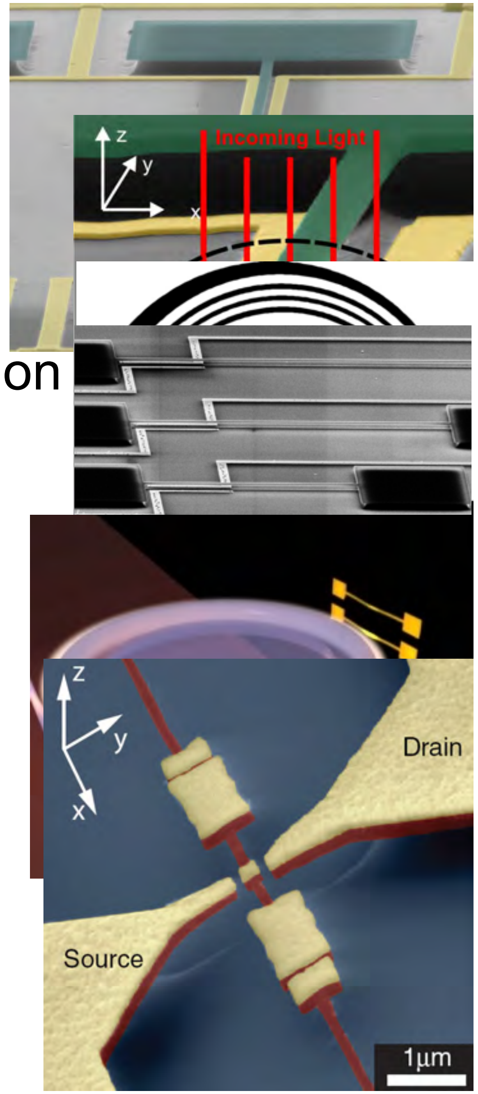

On-chip electrical gradient force transduction

in collaboration with

Quirin Unterreithmeier   Thomas Faust   Eva M. Weig

Actuating nanomechanical resonators

The pros and cons of common schemes

Magnetomotive

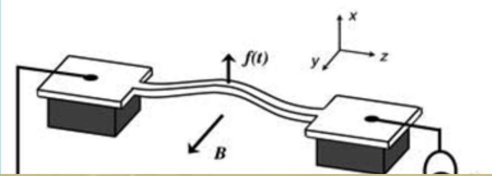

Capacitive

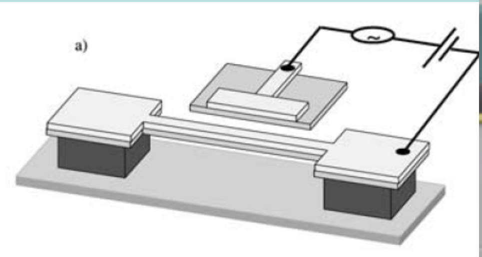

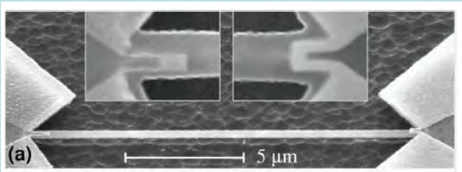

Electrothermal

Piezoelectric Material

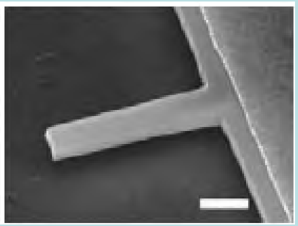

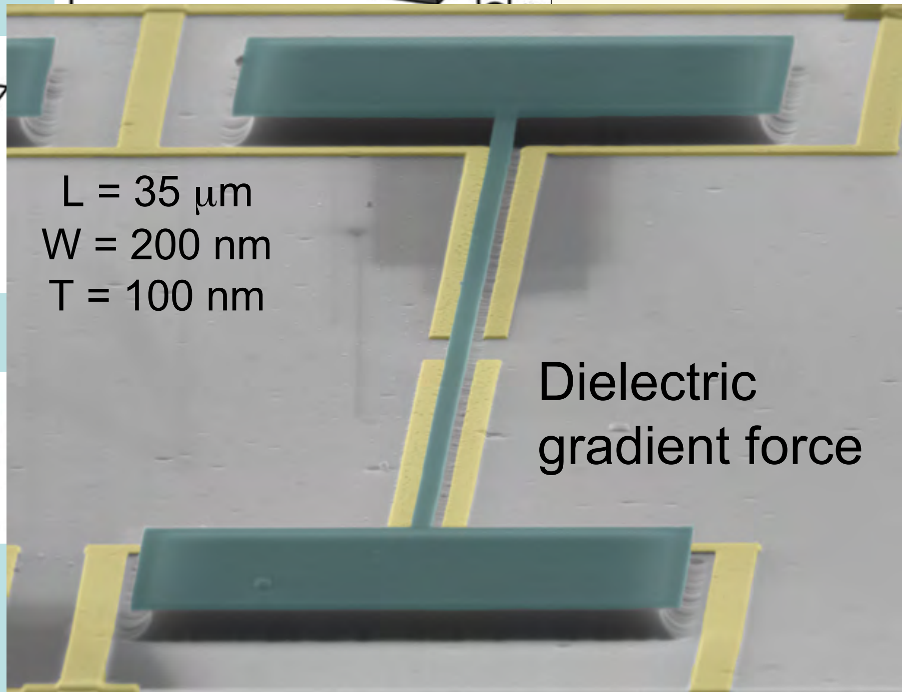

Photothermal

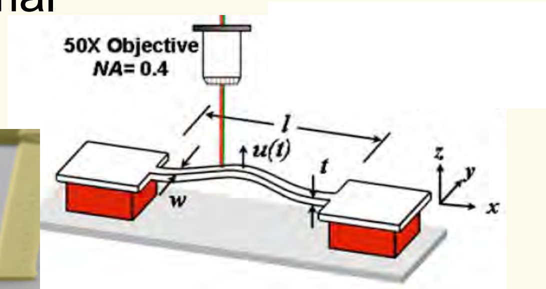

l. Phys. Lett. 88, 223104 (2006)

hybrid inertial drive

g. *Ekinci, Small1, 786 (2005)*

Local actuation

+ highly integrable
+ large bandwidth
- material & temperature constraints

External actuation

+ low material constraints (highest Q)
- not integrable
- high frequency limitations

The principle of dielectric actuation via a gradient force

A polarizable body subject to a gradient field will experience a force

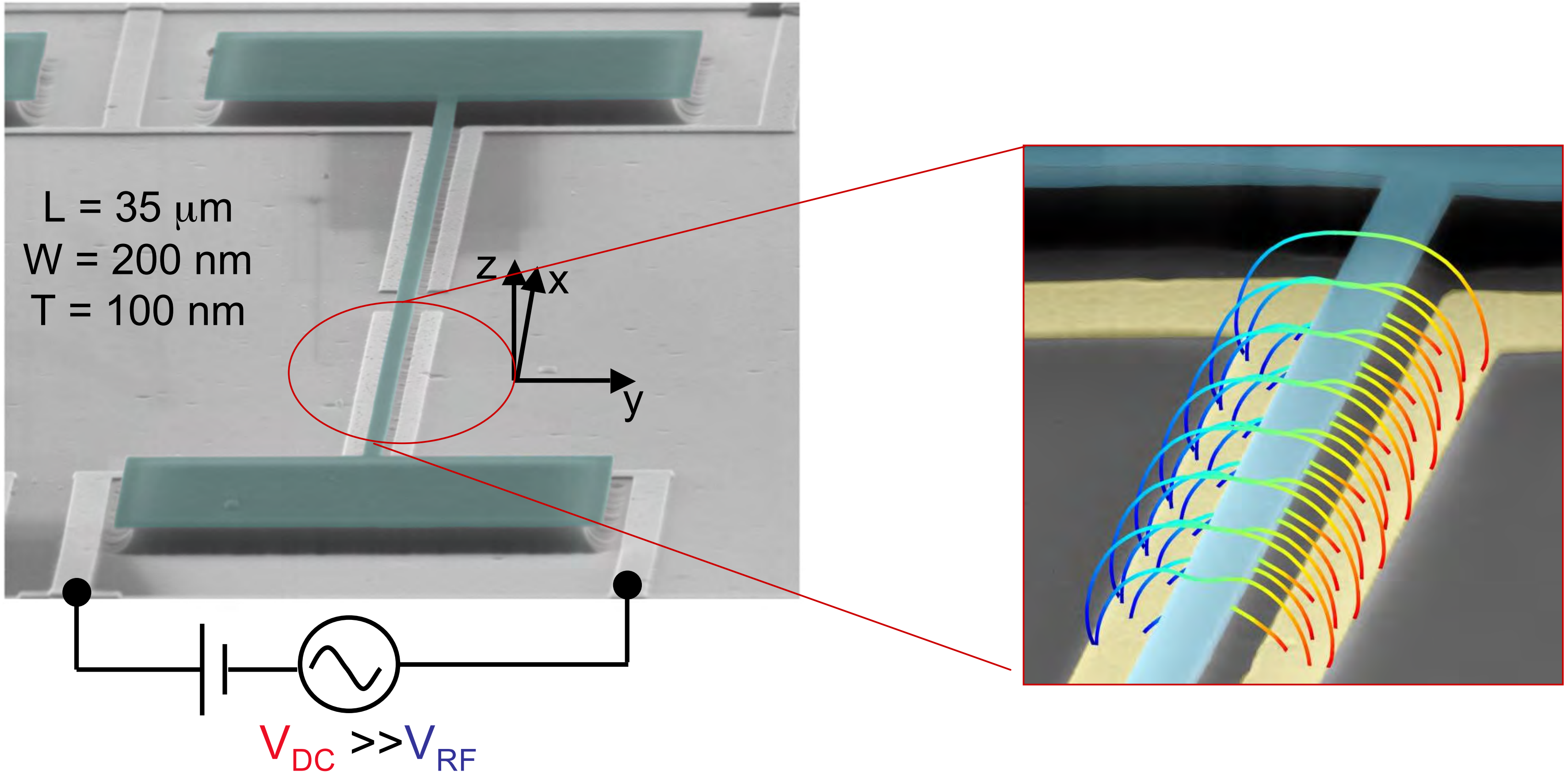

V_{DC} → polarization

V_{RF} → actuation

$$F_z = P_y \frac{\partial E_z}{\partial y} \propto E_y E_z$$

Q. Unterreithmeier, E. M. Weig, J. P. Kotthaus, Nature 458, 1001 (2009).

see also: S. *Schmid et al., Appl. Phys. Lett. 89, 163506 (2006)*

The principle of dielectric actuation

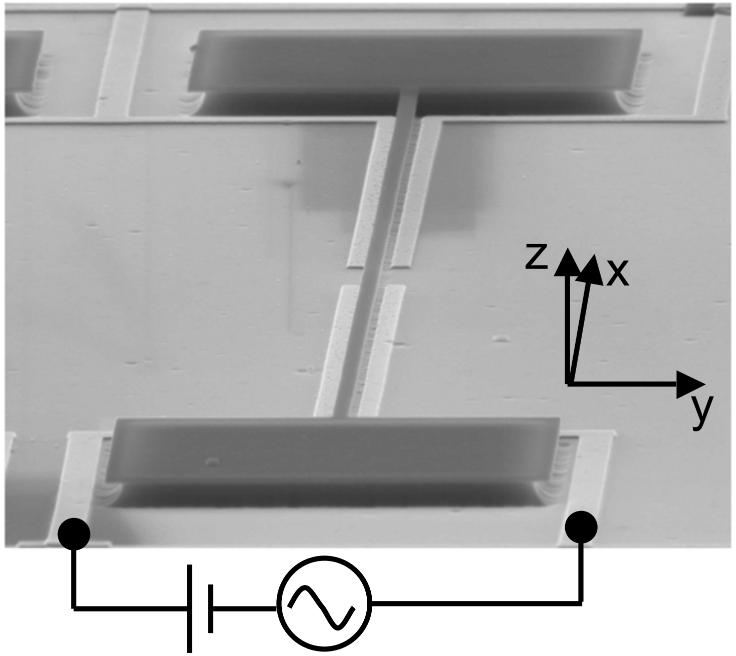

$V_{DC} >> V_{RF}$

DC voltage influences dipolar moment

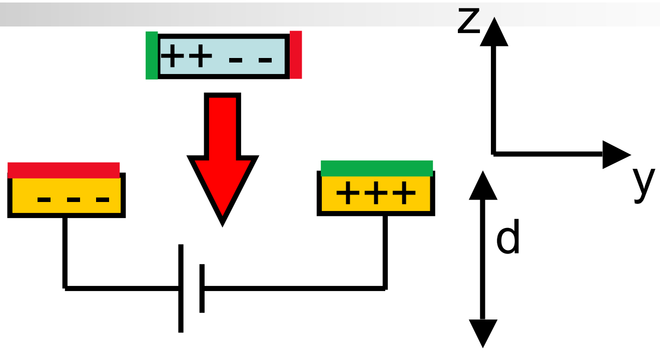

$$F_{DC} = P_y \frac{\partial E_y}{\partial z} \propto V_{DC}^2$$

RF voltage modulates attractive force

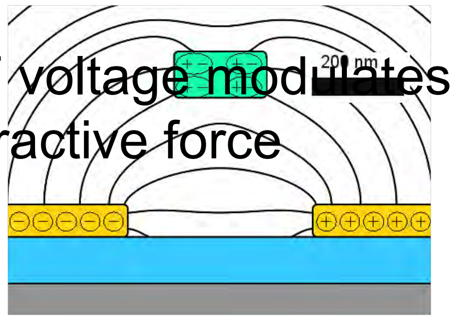

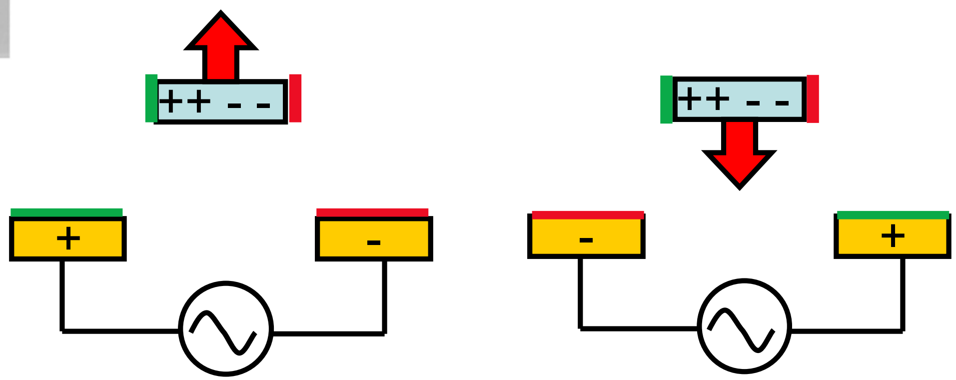

$$F_{RF} = P_y \frac{\partial E_y}{\partial z} \propto V_{DC} V_{RF}$$

Dielectric actuation with interferometric detection

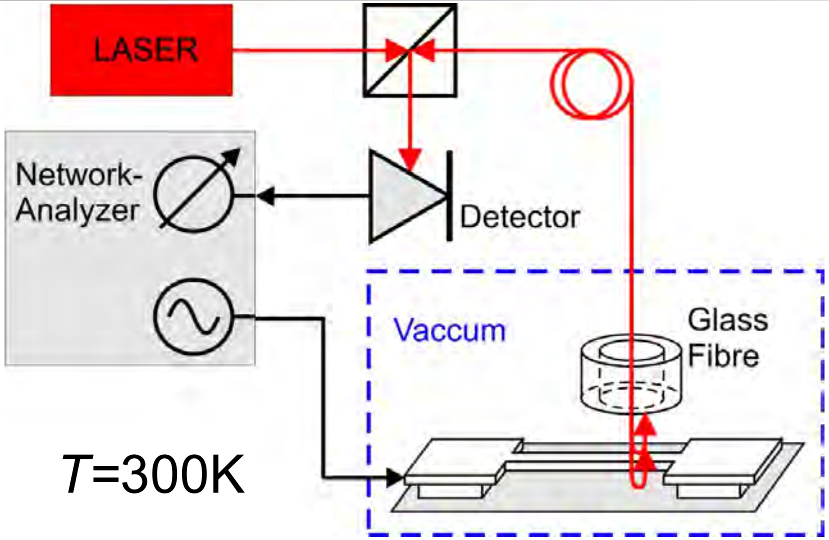

T=300K

V_{DC} = 2 V
V_{RF} = 0.2mV

$\omega_0/(2\pi)$ = 8 MHz
$Q = \omega_0/\Delta\omega_0$
= 150 000

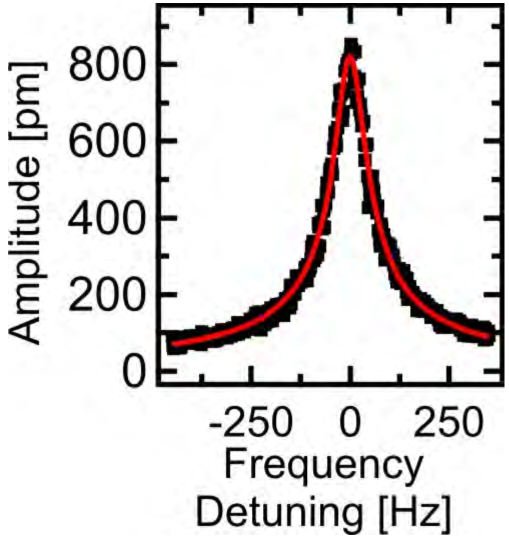

$$\frac{\partial^2}{\partial t^2} u[x,t] + \frac{\omega_0}{Q}\frac{\partial}{\partial t} u[x,t] + \omega_0{}^2 u[x,t] = \frac{F_z}{m}\cos[\omega t]$$

Displacement calibration through Brownian motion

$$\frac{1}{2}k_B T = \frac{1}{2}m\omega_0^2\langle x^2\rangle$$

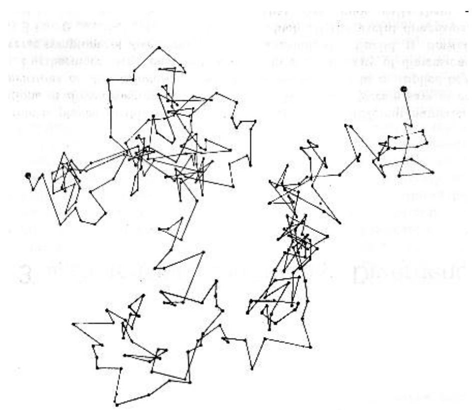

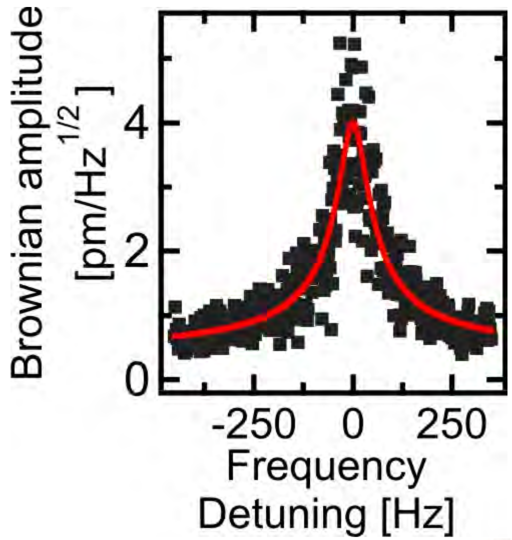

Dielectric actuation – DC tunabiliy

V_{RF}=0.2mV

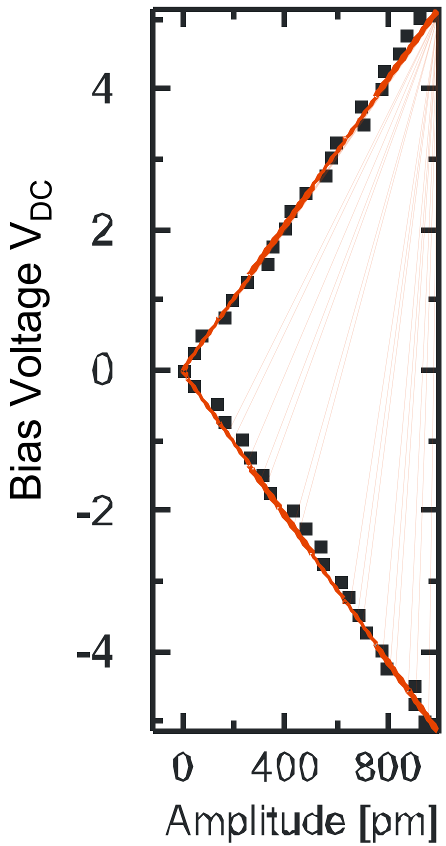

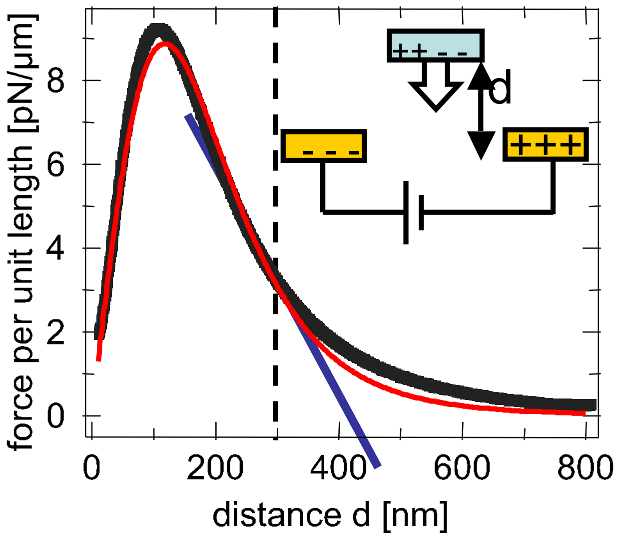

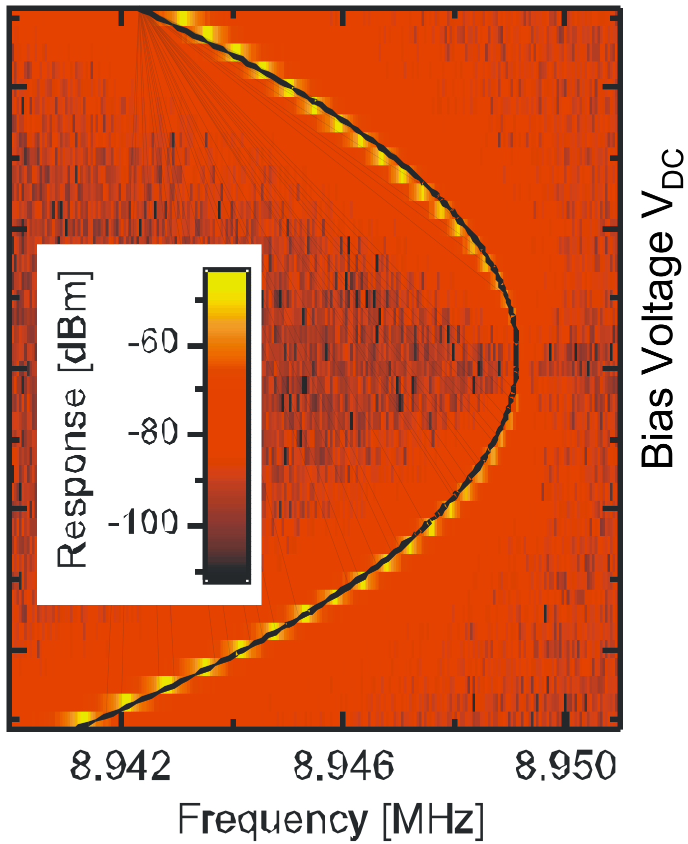

The force gradient counteracts the spring constant

$$F_{\mathrm{RF}} \propto V_{\mathrm{DC}} V_{\mathrm{RF}}$$

$$\frac{\partial F_{\mathrm{DC}}}{\partial z} \propto F_{\mathrm{DC}} \propto V_{\mathrm{DC}}^2$$

Tunability range ~1000 FWHM

Dielectric actuation of nanomechanical resonators

Combining the advantages of local and external actuation

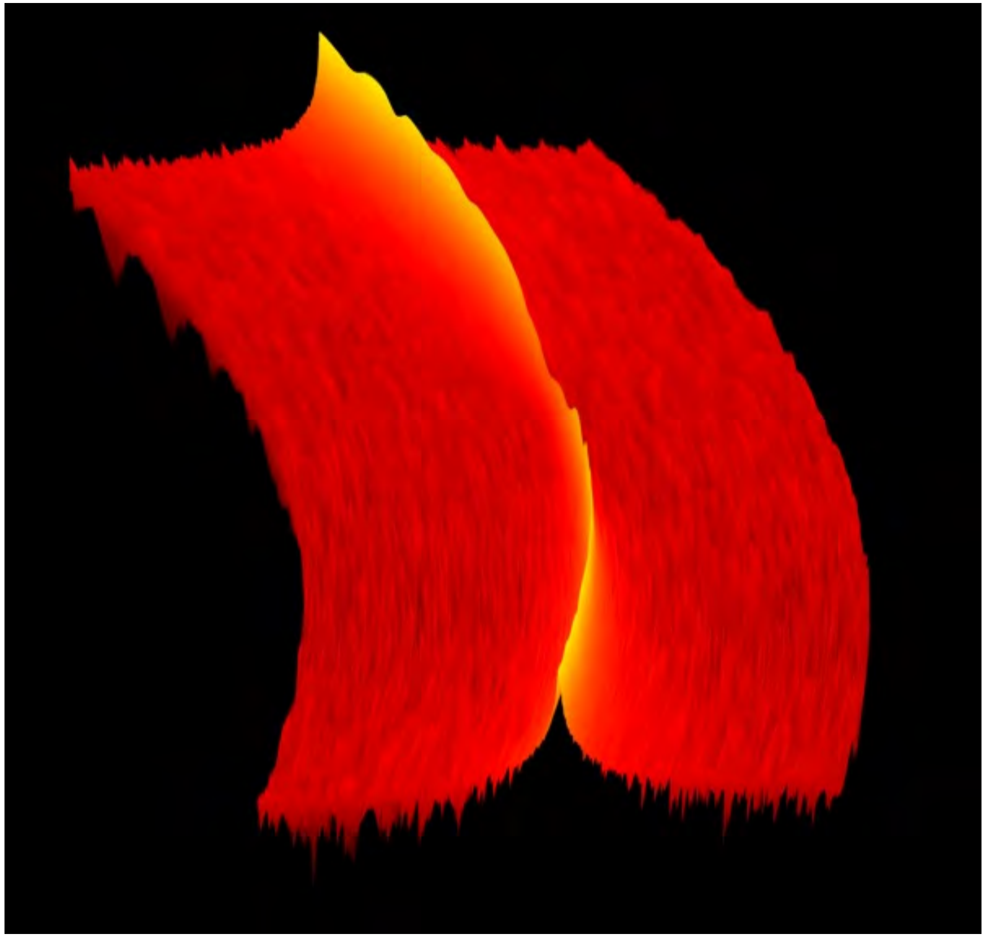

+ local, all-electronic, i.e. integrable

+ applicable to most materials (Q = 100,000 – 150,000)

+ polarization control via V_{DC}

+ efficient (V_{RF} > 5 µV)

+ scalable to high frequencies

$$R = 50\,\Omega$$
$$C_{mutual} = 1.5\,fF$$
$$\Rightarrow f_{cutoff} = 1/(2\pi R C_{mutual}) \approx 2\,THz$$

+ frequency tuning ~ V_{DC}^2
amplitude tuning ~ V_{DC}

Q. Unterreithmeier, E. M. Weig, J. P. Kotthaus, Nature 458, 1001 (2009).

Towards scalable on-chip detection

Representative presently employed detection schemes

Optical

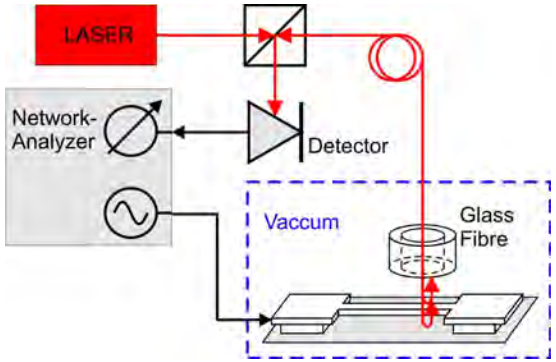

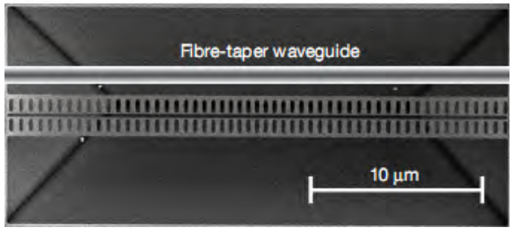

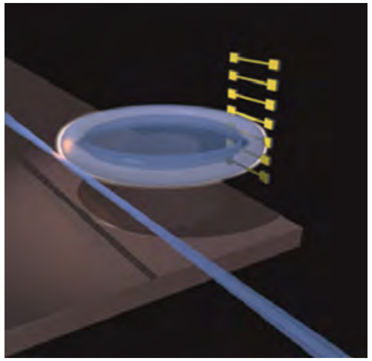

Electrical

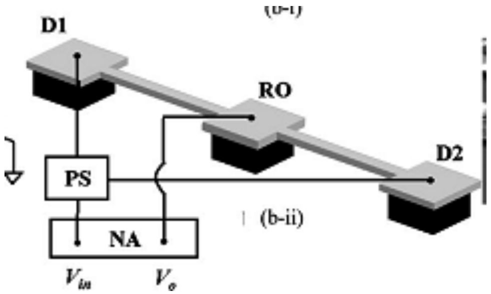

Magnetomotive

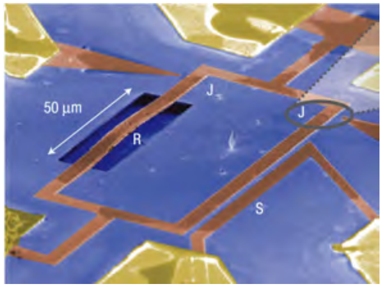

Flux-modulation

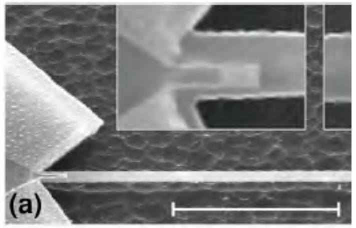

Piezoresistive

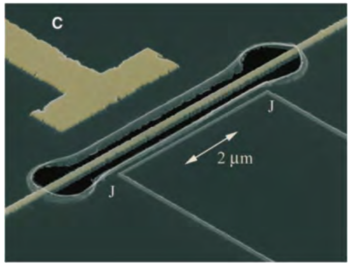

Single Electron Transistor

Parametric actuation

Self-oscillation without externally applied driving force

Modulate resonance frequency of the resonator at twice the resonance frequency:

$$\frac{\partial^2}{\partial t^2}u[x]+\frac{\omega_0}{Q}\frac{\partial}{\partial t}u[x]+\omega_0{}^2(1+\delta\sin(2\omega t))u[x]=0$$

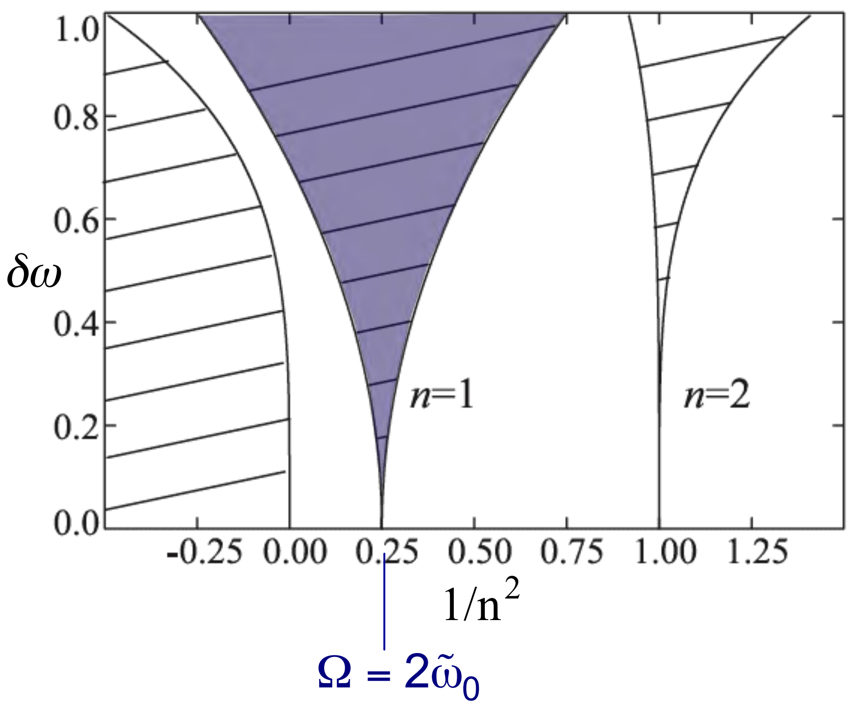

Instability and spontaneous self-oscillation for $\delta\omega > \frac{\tilde{\omega}_0}{Q}$.

Parametric actuation and dielectric detection

Modulating the resonance frequency at $2f_0$ via "V_{DC}" allows to invert the actuation principle

interferometric readout:

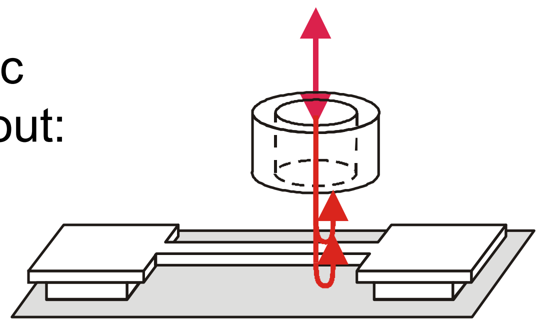

dielectric readout:

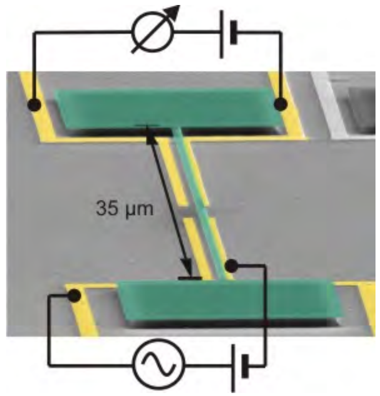

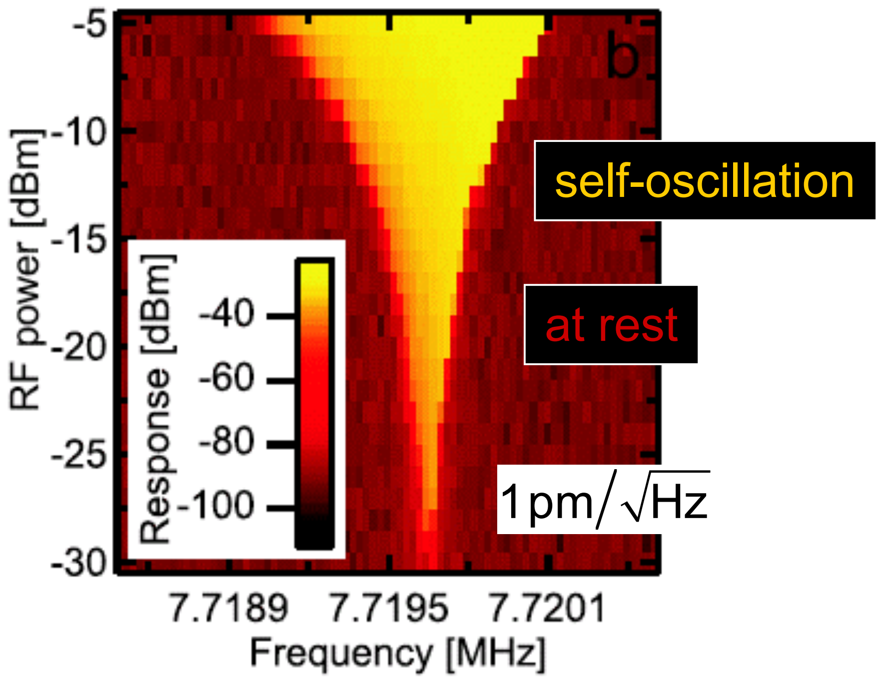

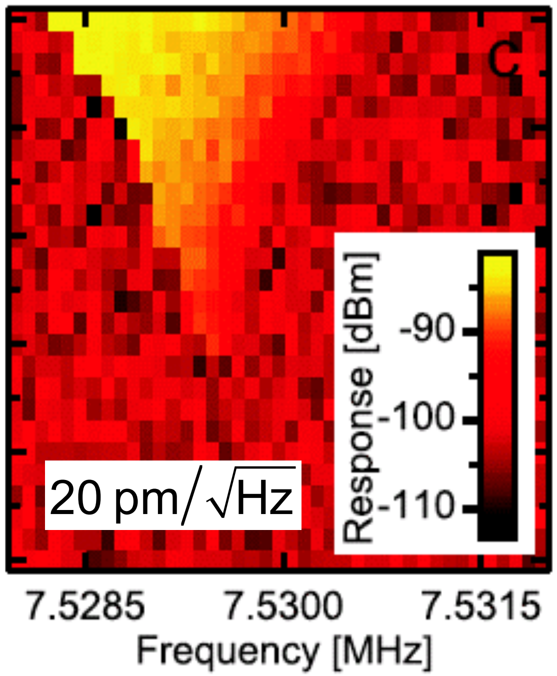

Concept of on-chip interferometric detection

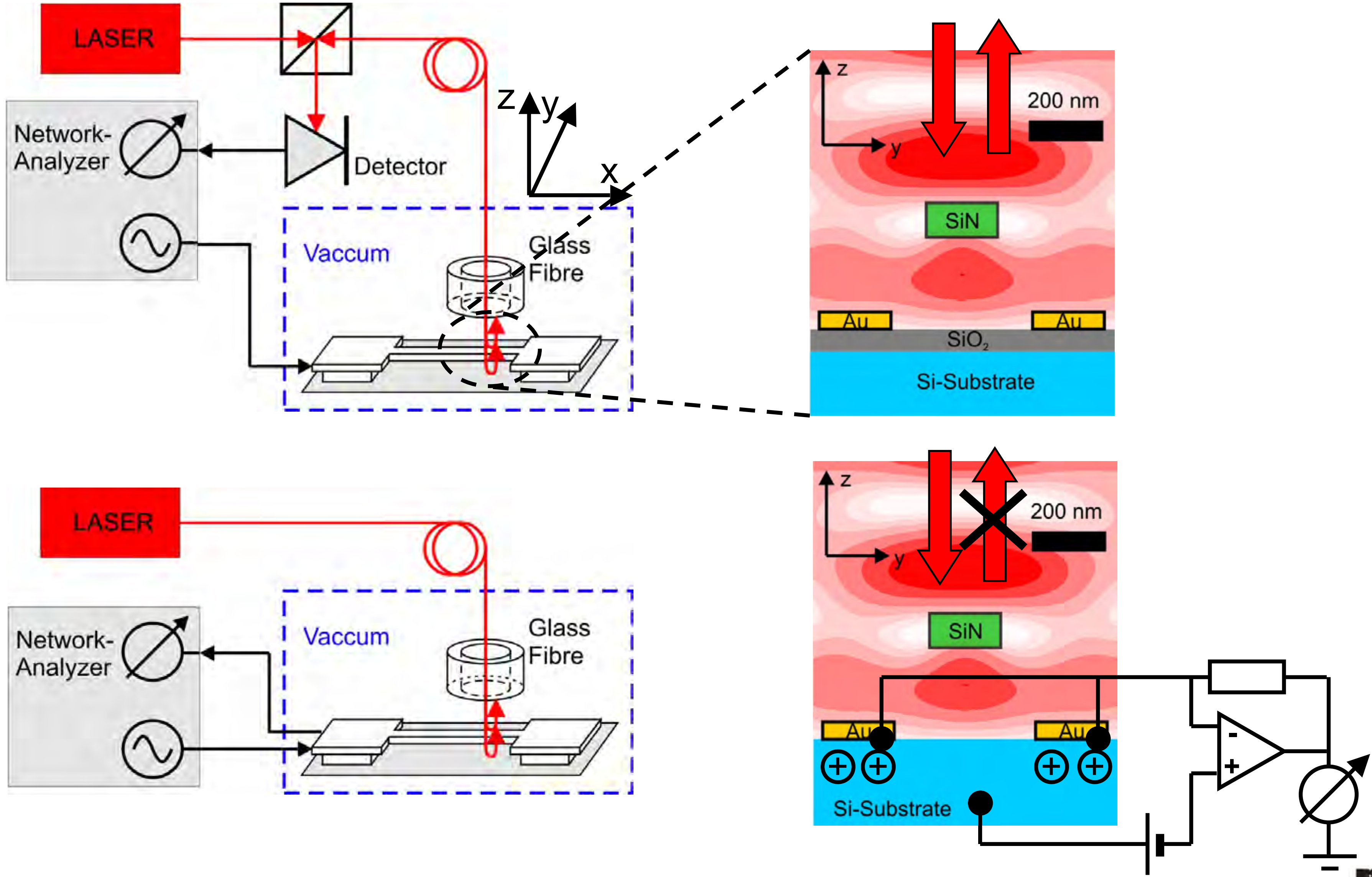

On-chip interferometric detection with Schottky photodiode

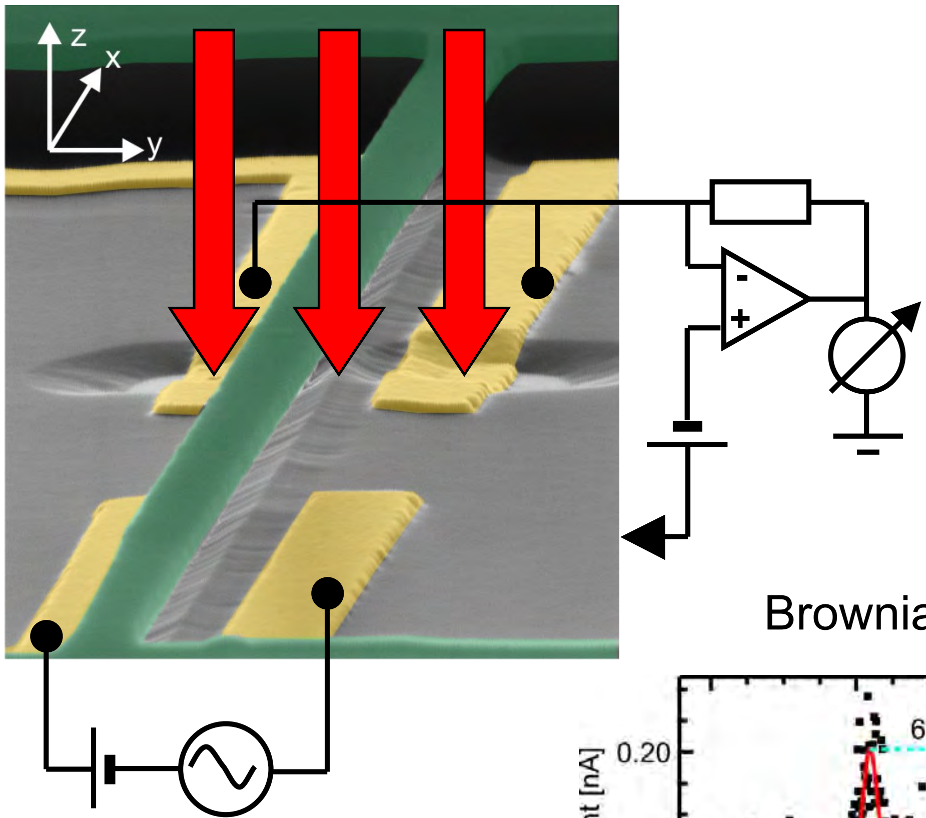

DC response

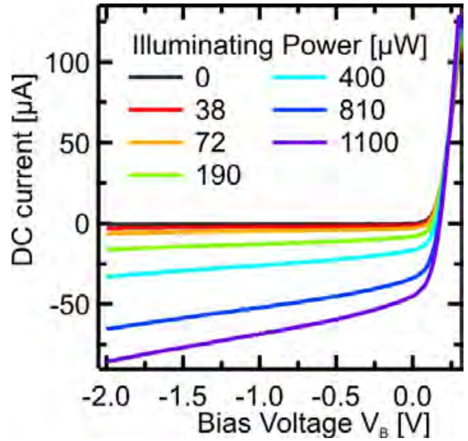

RF response

Brownian

Externally actuated

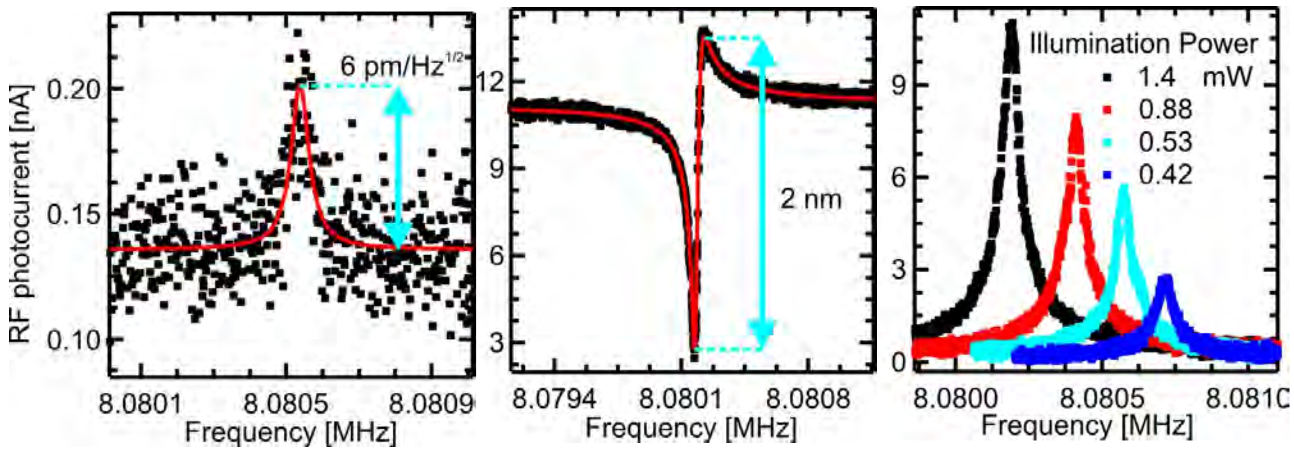

No Q-loading!
Non-Demolition

Q. Unterreithmeier, T. Faust, S. Manus, and J.P. Kotthaus
Nano Lett. 10, 887 (2010)

Feedback-stabilized self-exciting oscillator (PLL)

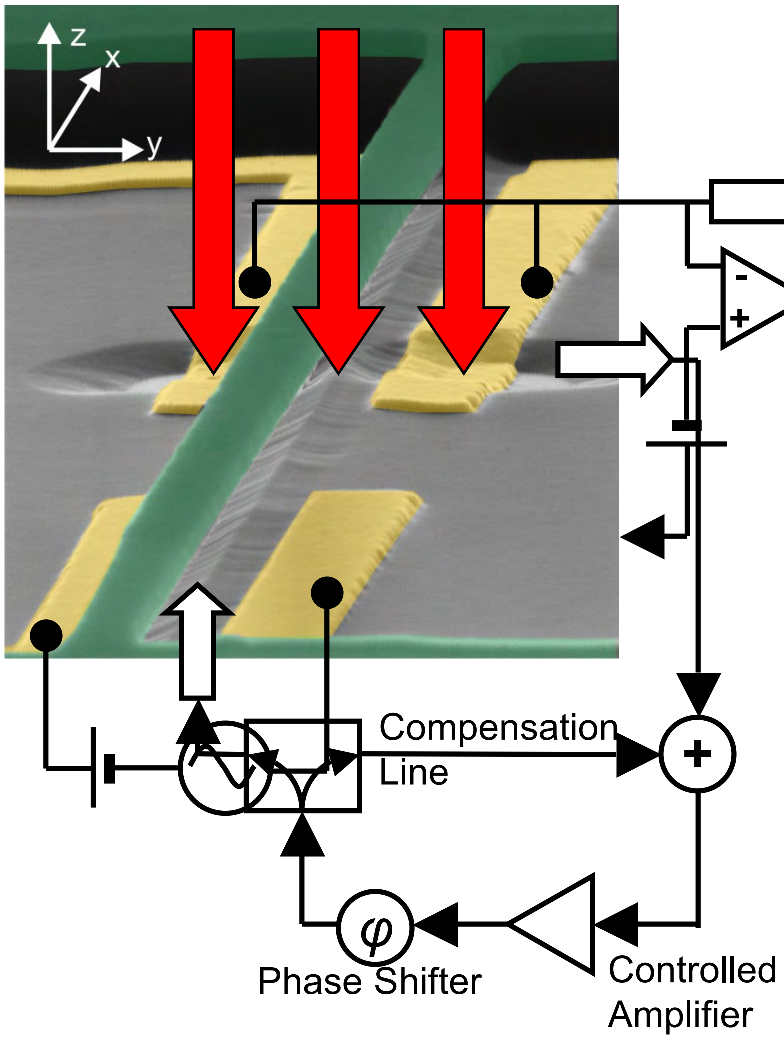

Self oscillation

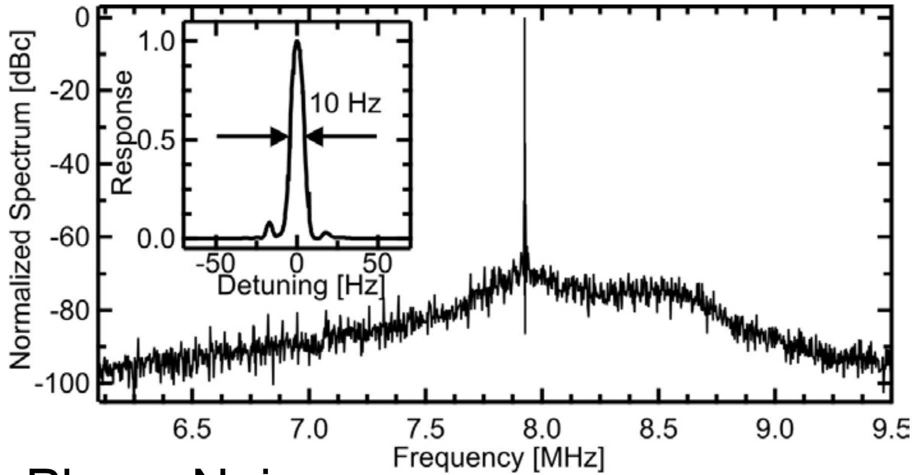

Phase Noise

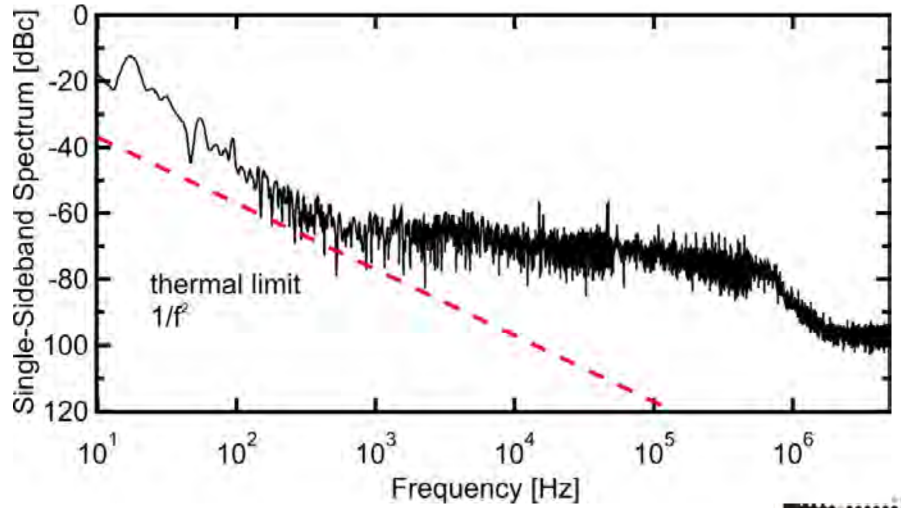

Q. Unterreithmeier, T. Faust, S. Manus, and J.P. Kotthaus
Nano Lett. 10, 887 (2010)

Non-linear nanomechanical oscillators - quasistatic behavior

$$\frac{\partial^2}{\partial t^2}u[x]+\frac{\omega_0}{Q}\frac{\partial}{\partial t}u[x]+\omega_0{}^2(1+\alpha u[x]^2)u[x]=\frac{F}{m}\cos[\omega t]$$

Equation of motion of a Duffing oscillator

$$u = a[\omega]\cos[\omega t+\gamma[\omega]]$$

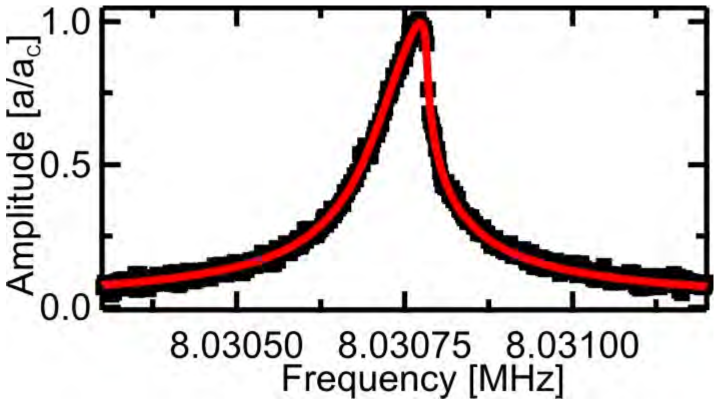

-> Fitting yields ω_0,Q,α

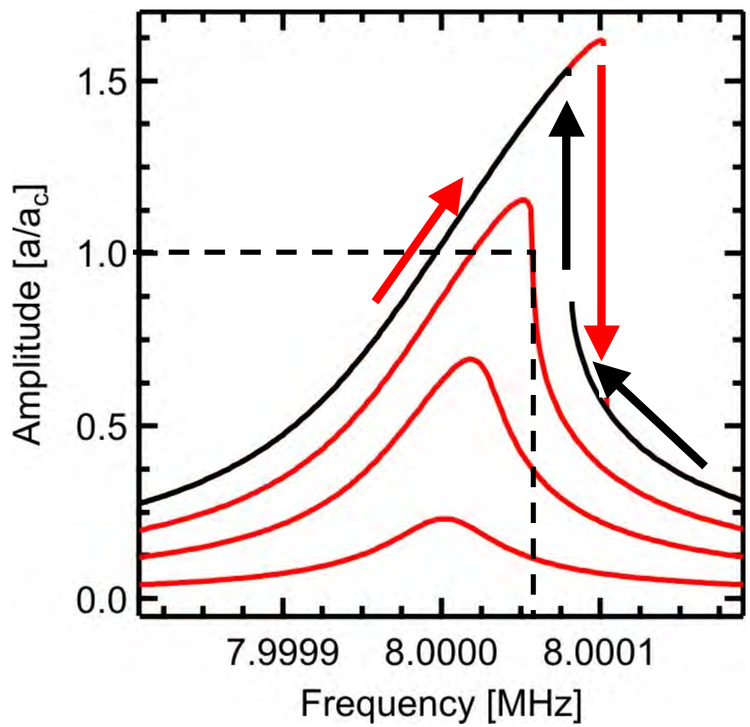

Nonlinear nanomechanics - dynamical behavior

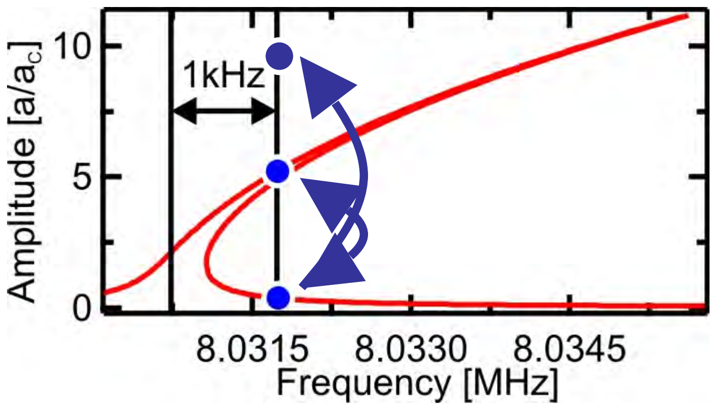

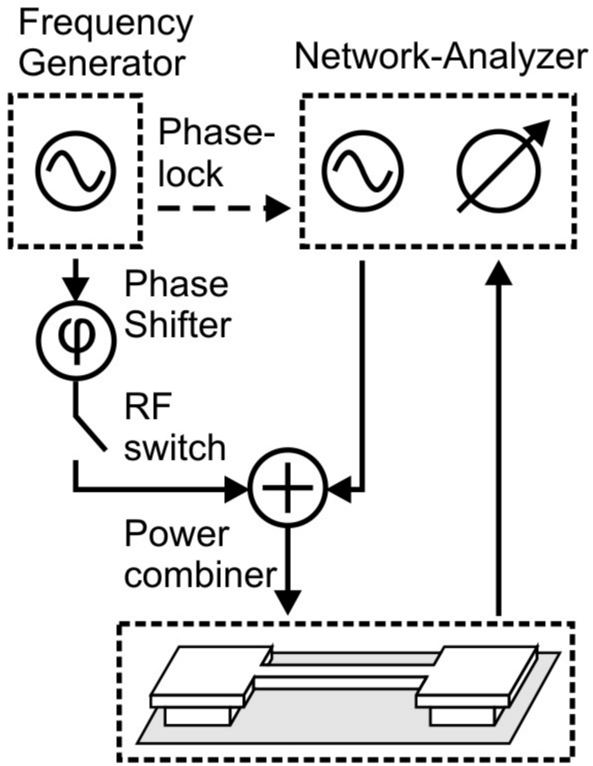

Driven resonator with
cw excitation at $f_0 + \sigma$ (σ =1kHz)

Fast switchable memory element
employing short resonant RF-pulses?

R. L. Badzey et al.,
Appl. Phys. Lett., **85**, 3587 (2004)

Nonlinear dynamics - relaxation into basins of attraction

Relaxation of the resonator driven continuously at frequency $f_0 + \sigma$
after excitation with strong rf pulse (~ 250 µs long, 18 x cw-amplitude)
of same frequency with amplitude a(t) and phase γ(t)

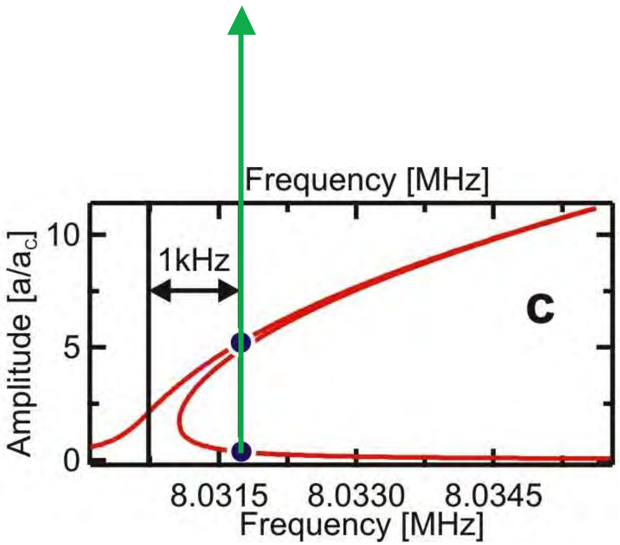

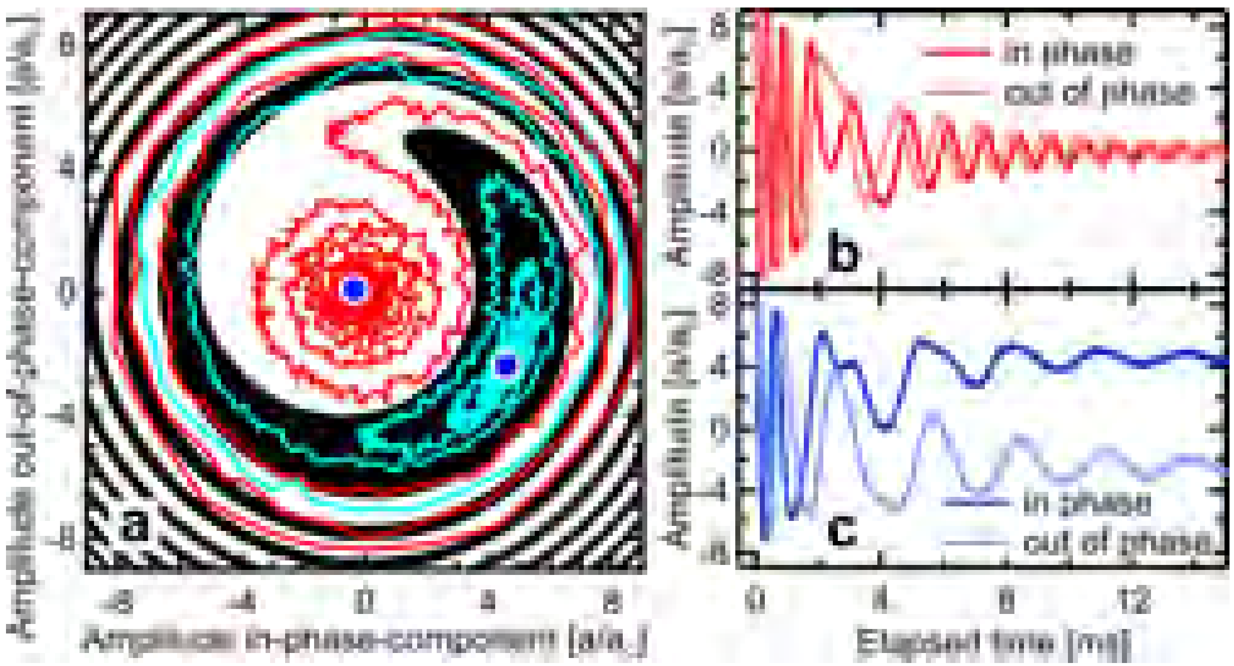

I. Kozinsky et al.,
Phys. Rev. Lett. **99**, 207201 (2007)

$$u[t] = a[t]\cos[\omega t + \gamma[t]]$$

$$= I[t]\cos[\omega t] + Q[t]\sin[\omega t]$$

In-phase component   Out-of-phase component

Q. Unterreithmeier, T. Faust, J.P. Kotthaus,
Phys. Rev. B **81**, 241405(RC) (2010)

Time evolution during application of RF pulse

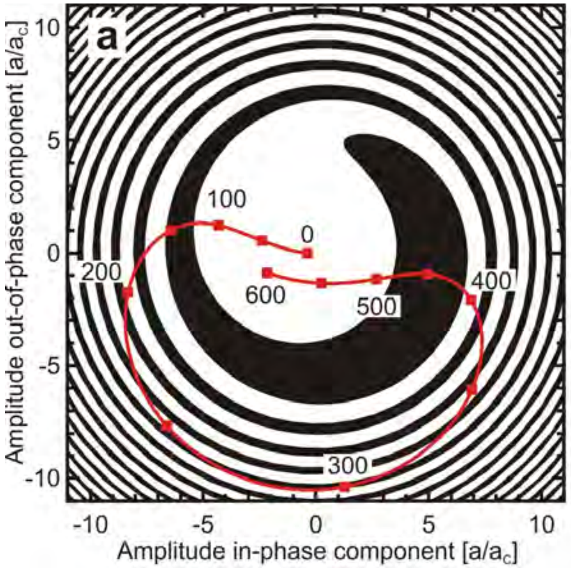

Predicted time evolution vs.

pulse duration Δt (in μs) at given phase φ

Δt and φ are systematically varied

$$\dot{a}(t) = -\frac{2\pi f_0 a(t)}{2Q} + \frac{k \sin(\gamma(t))}{4\pi f_0}$$

$$\dot{\gamma}(t) = 2\pi\sigma - \frac{3\alpha_3 a(t)^2}{16\pi f_0} + \frac{k\cos(\gamma(t))}{4\pi f_0 a(t)}$$

Experiment Simulation

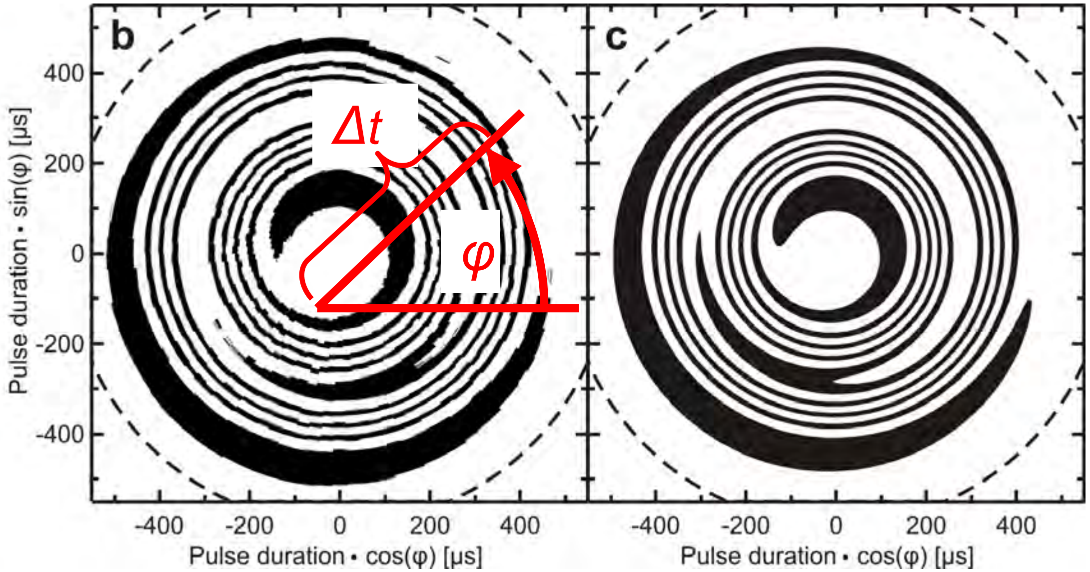

Measurement Protocol:

Final state vs. duration Δt and phase φ of RF pulse

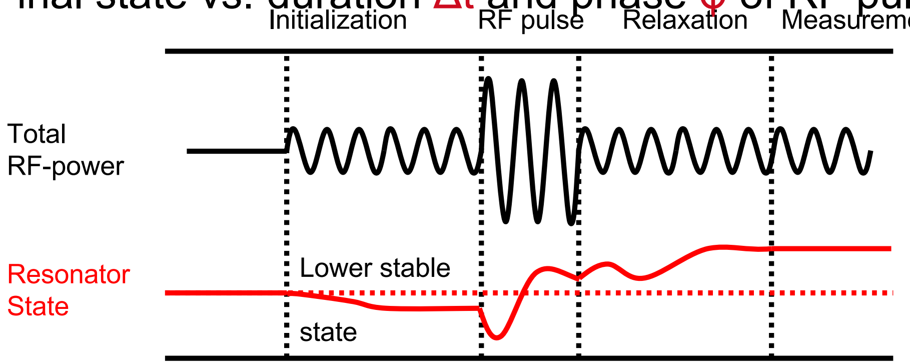

A non-adiabatically driven NEMS switch

on route to a NEMS memory

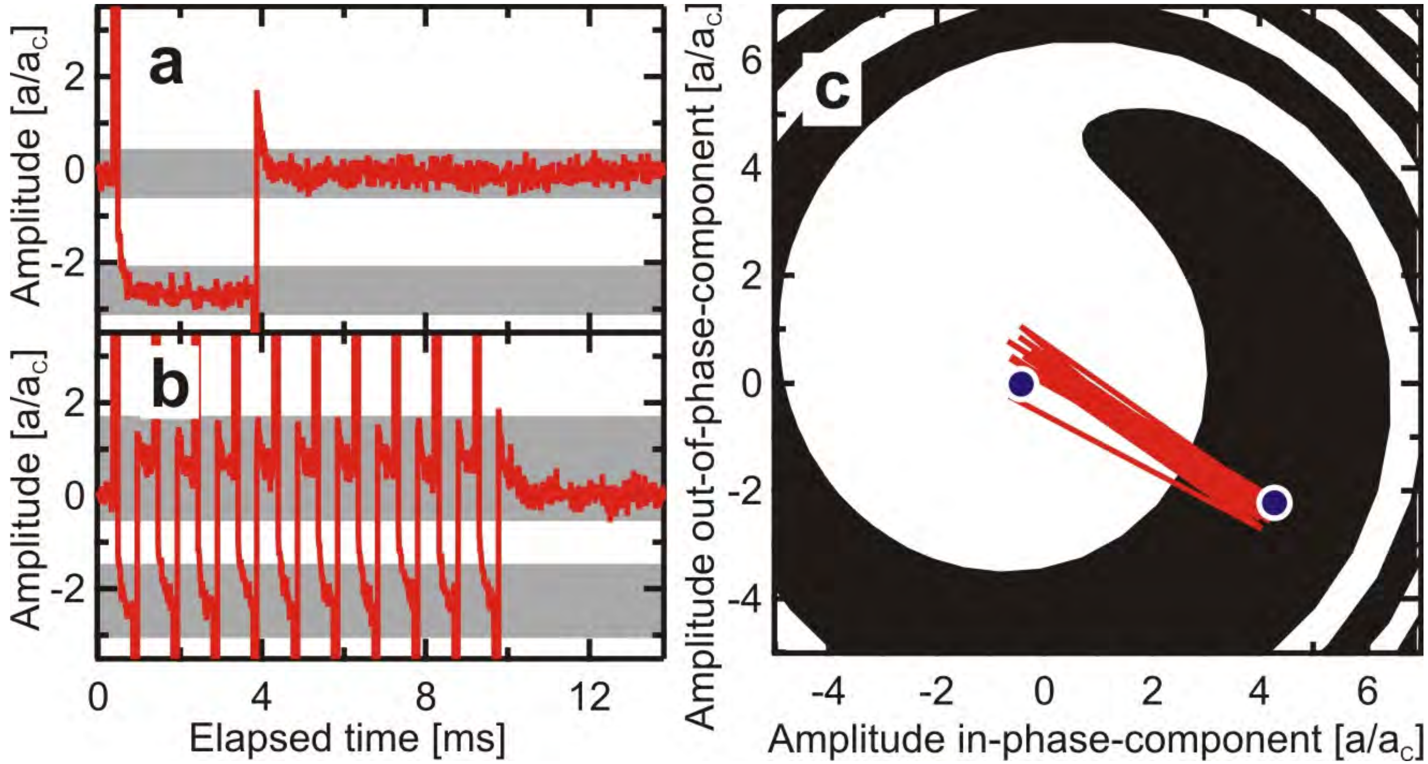

pulse duration 80 µs and repetition rate 1kHz, resonator relaxation time ~ 10 ms

-> switching beyond relaxation
(10^3 speed improvement)

Q. Unterreithmeier, T. Faust, J.P. Kotthaus,
Phys. Rev. B **81**, 241405(RC) (2010)

Damping: Quality factors of highly stressed beams

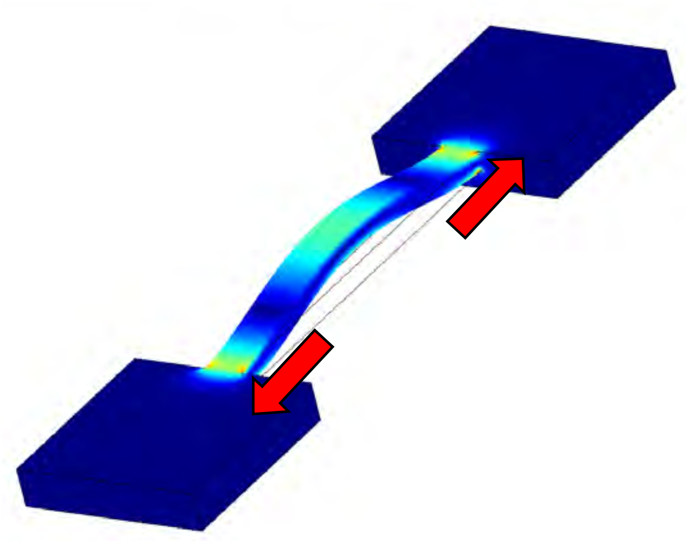

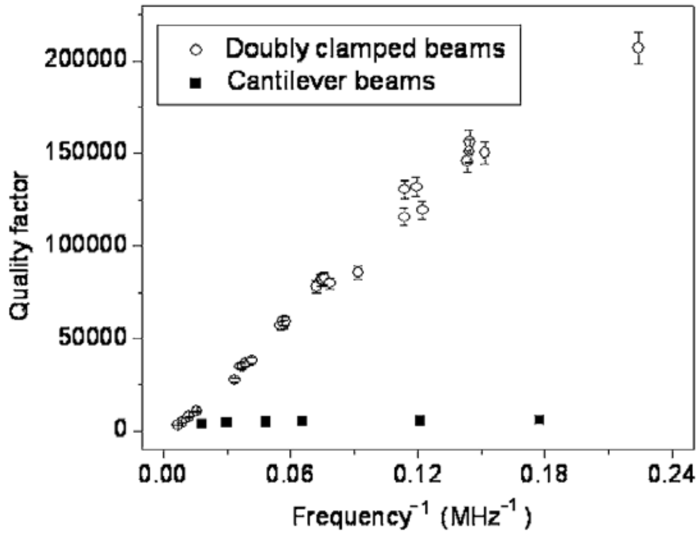

Mechanical quality factor

$$Q = 2\pi \frac{\text{energy stored}}{\text{energy loss per oscillation}}$$

-> Stress increases Q

S. Verbridge et al., J. Appl. Phys. **99**, 124304 (2006)

Mechanism?

Exploring length and mode-dependence of Q-factor

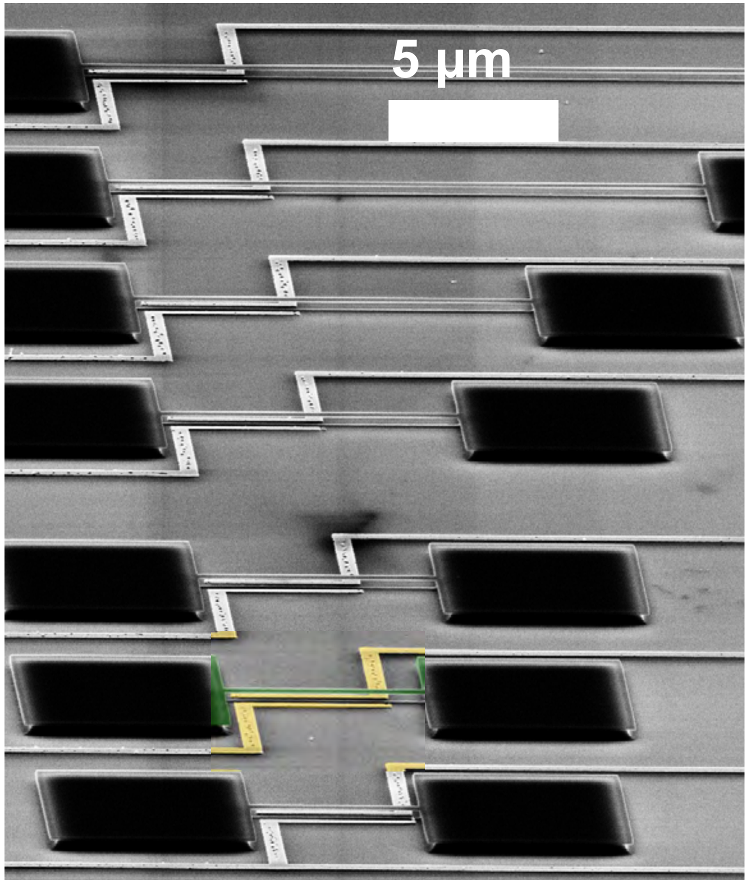

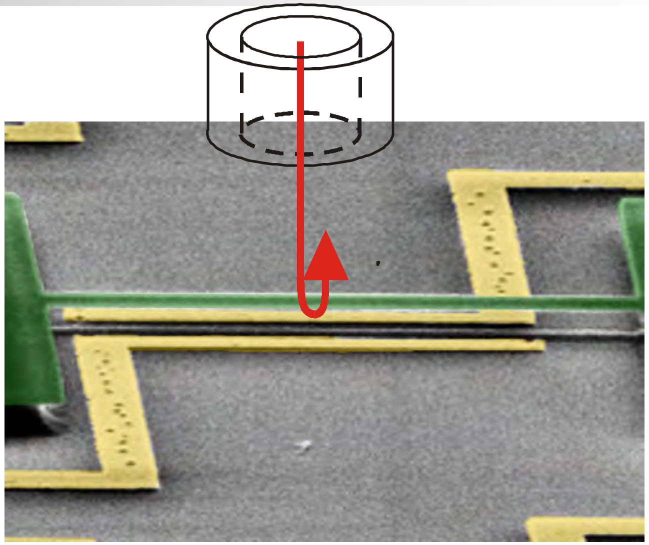

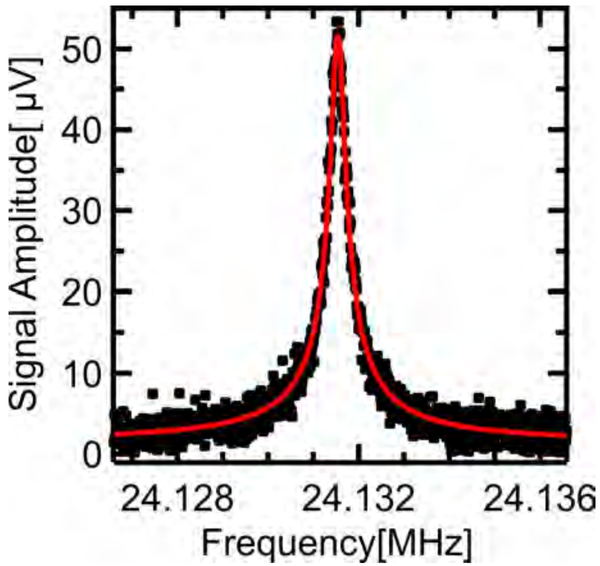

f, *Q* for different
-> mode number
-> beam length

Exploring frequency scaling and damping of harmonics

Each node of a vibrational modes yields a phase reversal:

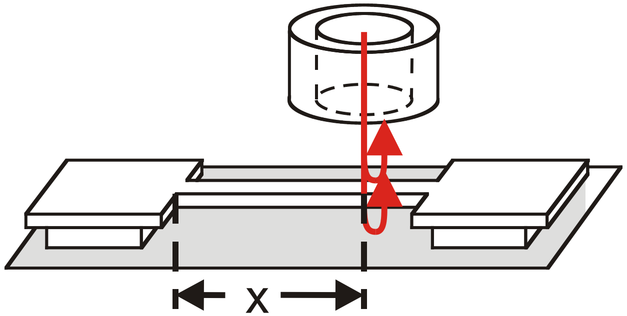

n = 1, n = 2, n = 3, n = 5, n = 7

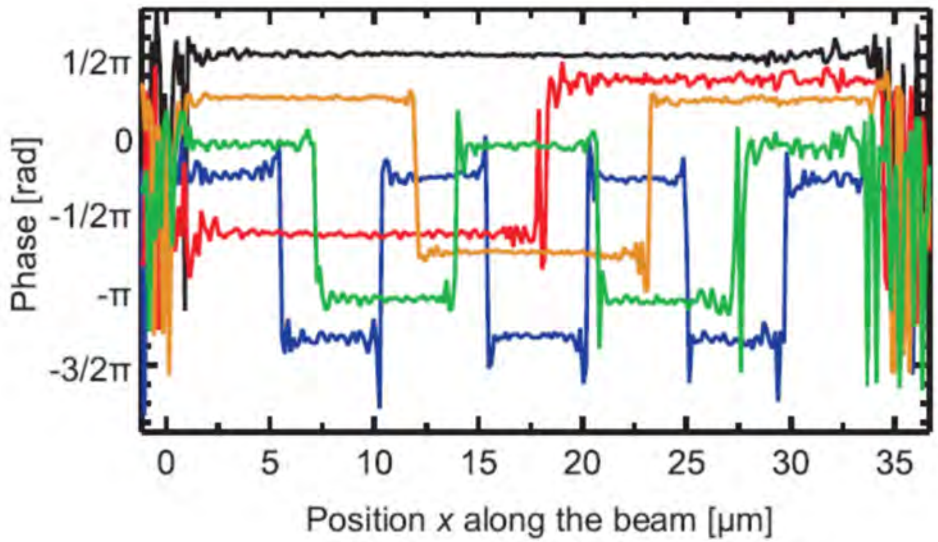

Q. Unterreithmeier, S. Manus, J. P. Kotthaus, Appl. Phys. Lett. 94, 263104 (2009)

- Bending rigidity: f α n^2

- String-like: f α n

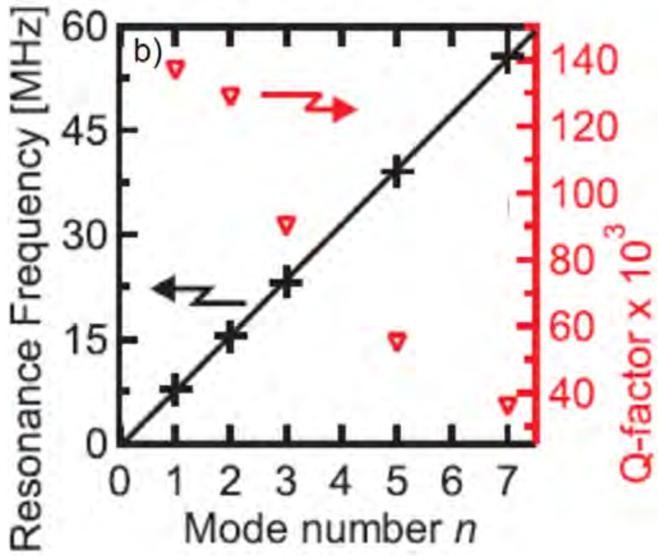

Resonance frequency versus harmonic mode

$$\frac{1}{12} E h^2 \frac{\partial^4}{\partial x^4} u_n[x] - \sigma_0 \frac{\partial^2}{\partial x^2} u_n[x] - \rho (2\pi f_n)^2 u_n[x] = 0$$

Bending rigidity — Beam elongation

$$\frac{\partial}{\partial x} u_n[\pm l/2] = u_n[\pm l/2] = 0$$

Rigid clamping points

Continuum mechanics with:
u_n: Beam displacement
h: Beam height
ρ: Density
f_n: Frequency (n-th Mode)
l: Beam length

yields:
E: Young's modulus
σ_0: Pre-Stress

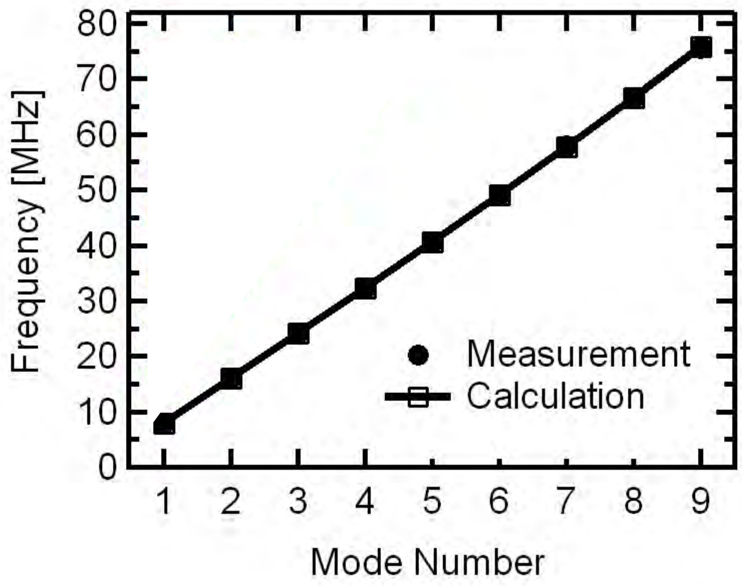

E = 160 GPa
σ_0= 830 MPa fit parameters

A simple single parameter damping model

consistent with experimental findings

Strain caused by displacement

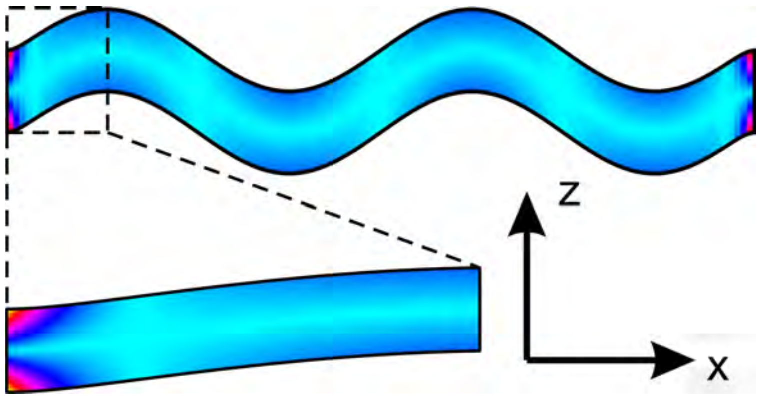

Strain ε and stress σ are out-of-phase

-> Complex Young‘s modulus

$E = E_1 + i\, E_2$

-> Energy loss per oscillation

$$\Delta U = \int_V dV \pi E_2 \varepsilon[x,z]^2$$

Assumption:

E_2 independent of x, mode, length

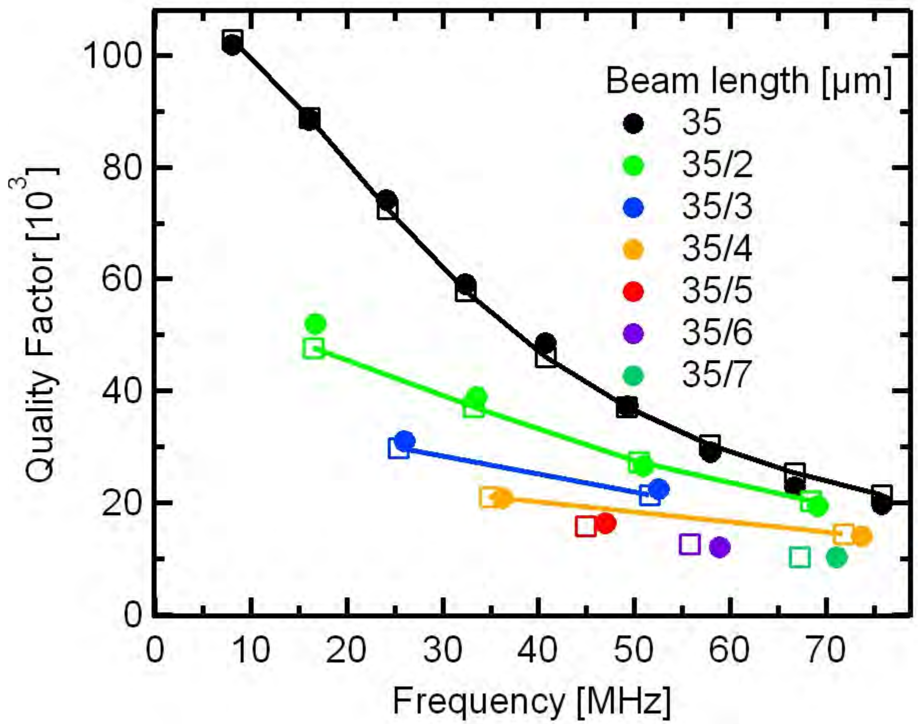

Q. Unterreithmeier, T. Faust, J. P. Kotthaus, Phys. Rev. Lett. 105, 027205 (2010)

Elastic energy and mechanical quality factor vs stress

Unstressed Beam

$$U = \int_V dV \frac{1}{2} E_1 \varepsilon[x,z]^2$$

$$\Delta U = \int_V dV \pi E_2 \varepsilon[x,z]^2 \qquad Q = \frac{\mathrm{Re}(E)}{\mathrm{Im}(E)}$$

-> mode-independent *Q*

Stressed Beam

-> rigidity -> Young‘s modulus
-> elongation -> external stress

$$U_{\text{elongation}} = \frac{1}{2}\sigma_0 wh \int_l dx(\partial/(\partial x) u[x])^2$$

$$U_{\text{rigidity}} = \frac{1}{24} E_1 wh^3 \int_l dx(\partial^2/(\partial x)^2 u[x])^2 \propto \Delta U$$

Q. Unterreithmeier, T. Faust, J. P. Kotthaus,
Phys. Rev. Lett. 105, 027205 (2010)

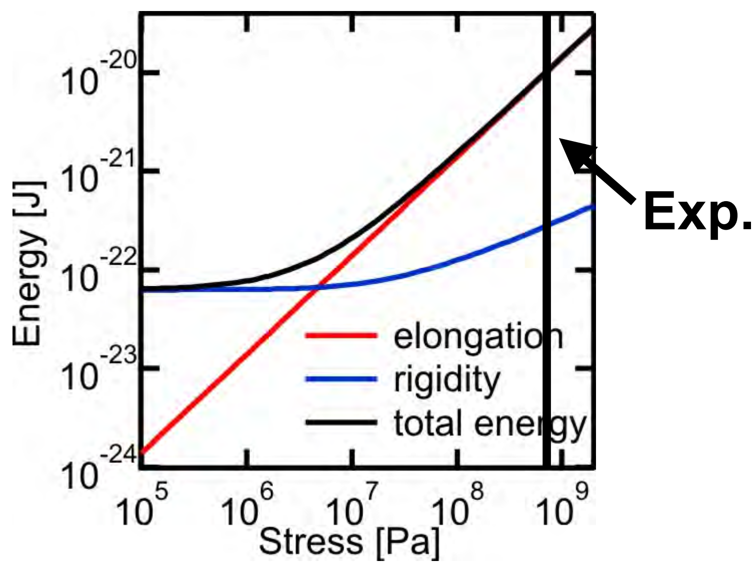

-> stress increases stored energy
-> stress does not change local energy loss very much

-> higher mechanical *Q*
dominated by increased stored energy and not by reduced damping

Contribution of clamping losses to damping

Irradiation of acoustic waves into the substrate

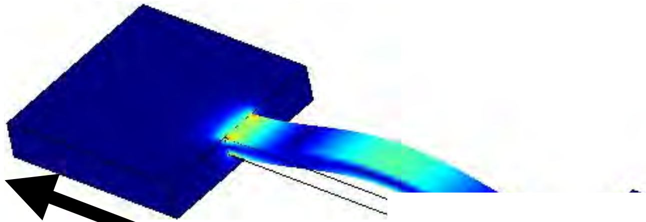

Symmetric mode
monopole

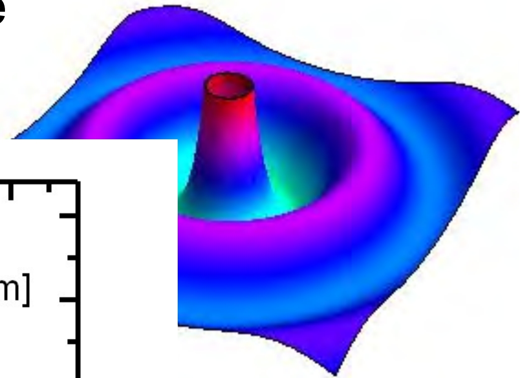

length s=35µm

<< wavelength λ

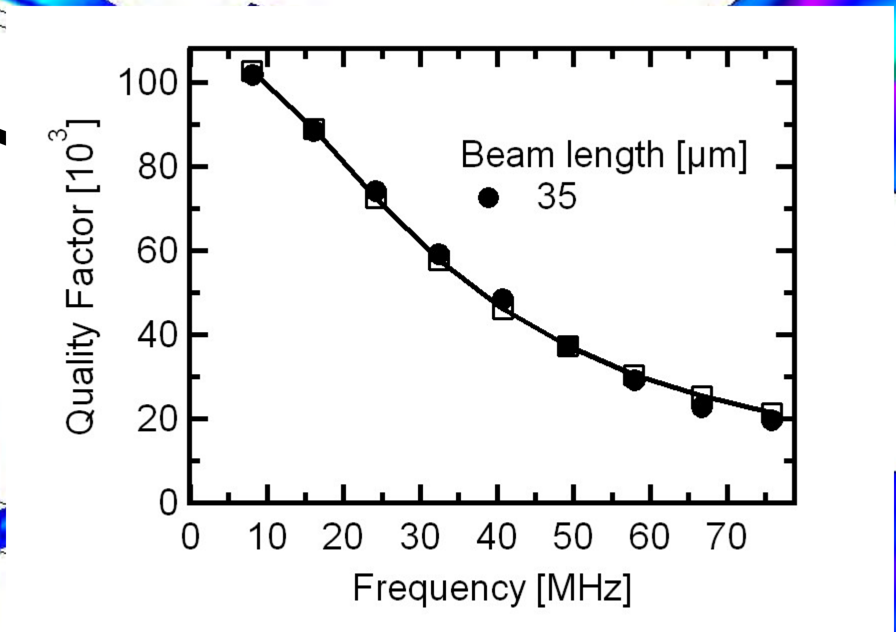

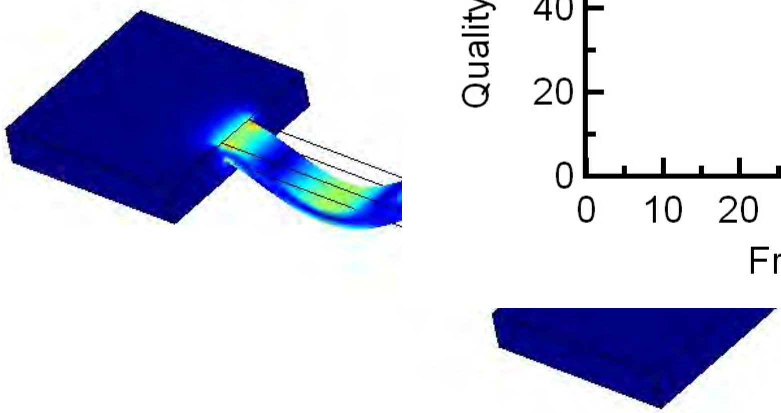

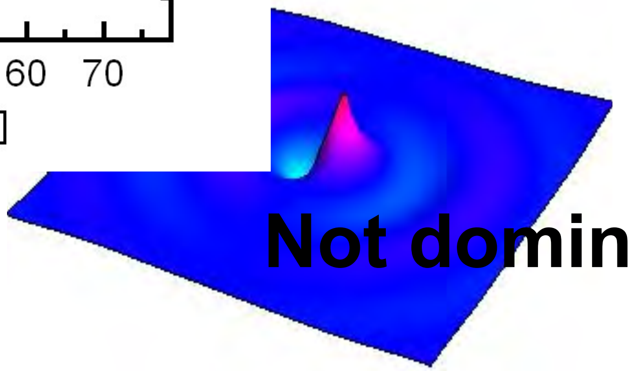

Not dominant!

I.Wilson-Rae,
Phys. Rev. B**77**, 245418 (2008)

Contribution of thermoeleastic damping

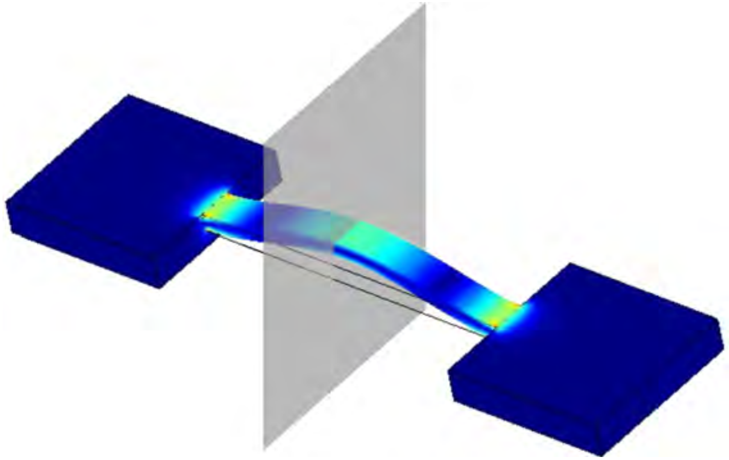

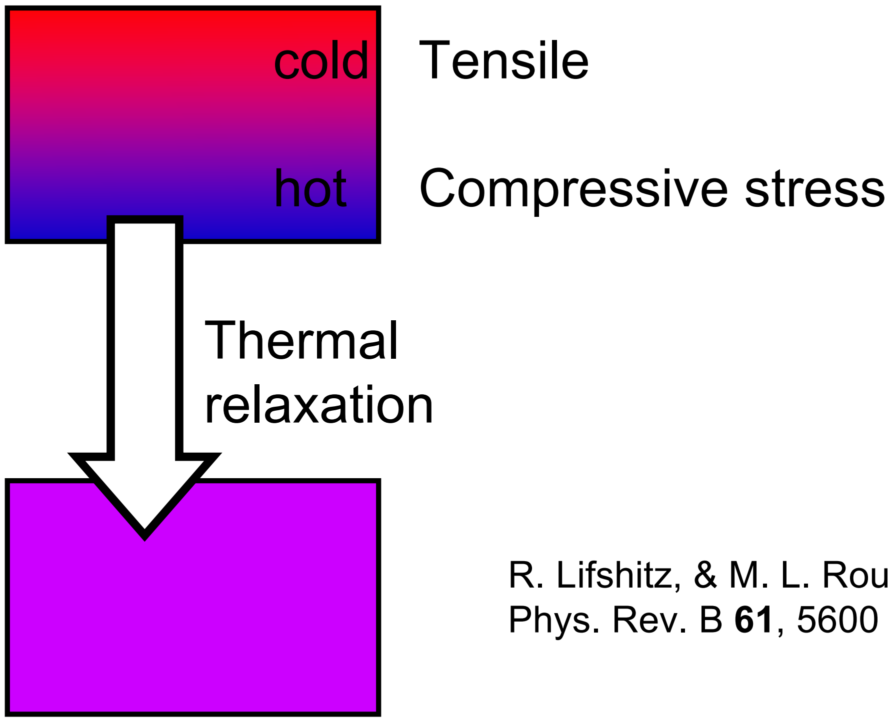

R. Lifshitz, & M. L. Roukes,
Phys. Rev. B **61**, 5600 (2000)

-> Very small damping
-> Thermal relaxation faster than oscillation (-> frequency dependence)

Not dominant!

Contribution of the Akhiezer effect to damping

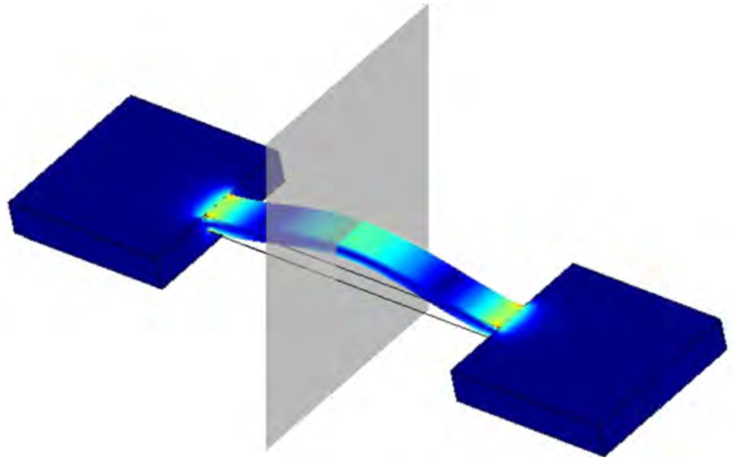

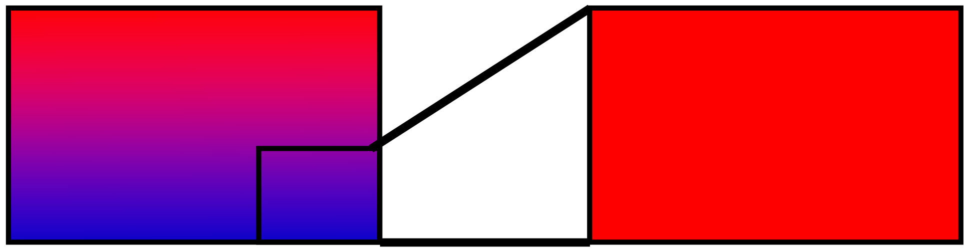

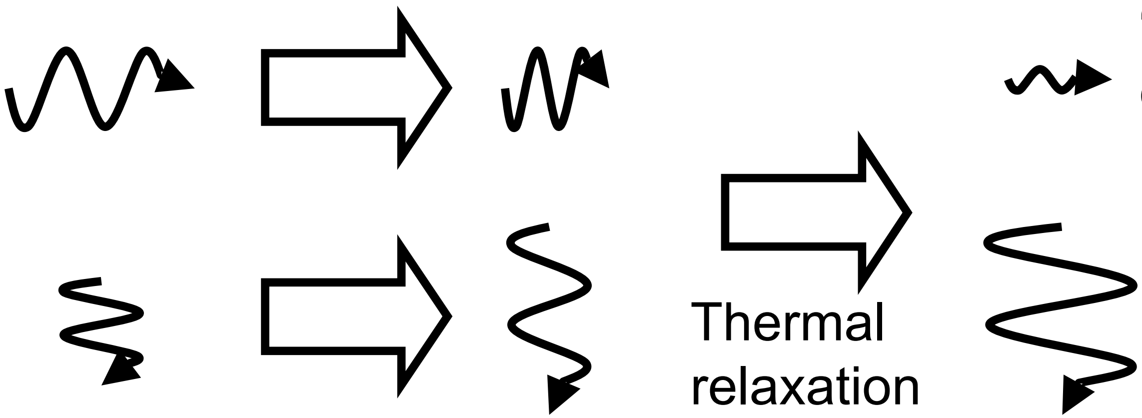

"Akhiezer damping" < "Thermoelastic damping"

Kiselev, A. A. & Iafrate, G. J.,
Phys. Rev. B, **77**, 205436 (2008)

Different phonon modes are affected differently by strain
-> each mode has different temperature

Not dominant!

Damping via localized defect states

Long-wavelength oscillatory mode decays into
energetically degenerate manifold of localized states

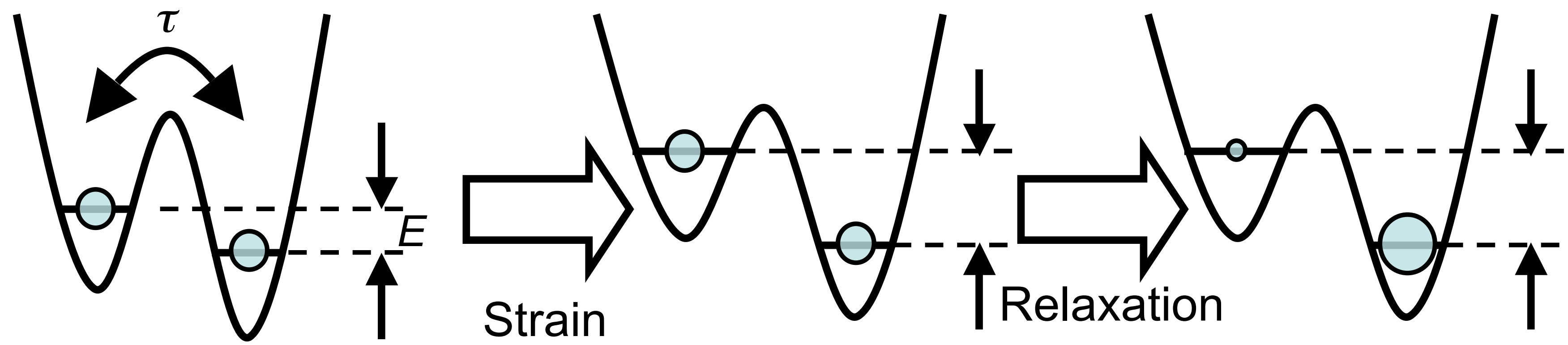

broad distribution in
E,τ
high temperature limit
-> frequency independent
energy loss

J. Jaeckle, Z. Phys. **257**, 212 (1972)

Magnitude well in the
“glassy range“ at
“medium temperature“

Most likely!

D. R. Southworth et al.,
Phys. Rev. Lett., **102**, 225503 (2009)
R. Pohl, et al. Rev. Mod. Phys., **74**, 991 (2002)

Gradient forces in NanoOptoMechanical Systems

Recent examples of actuation, transduction and back-action

J. D. Thompson et al., Nature 452, 72 (2008)

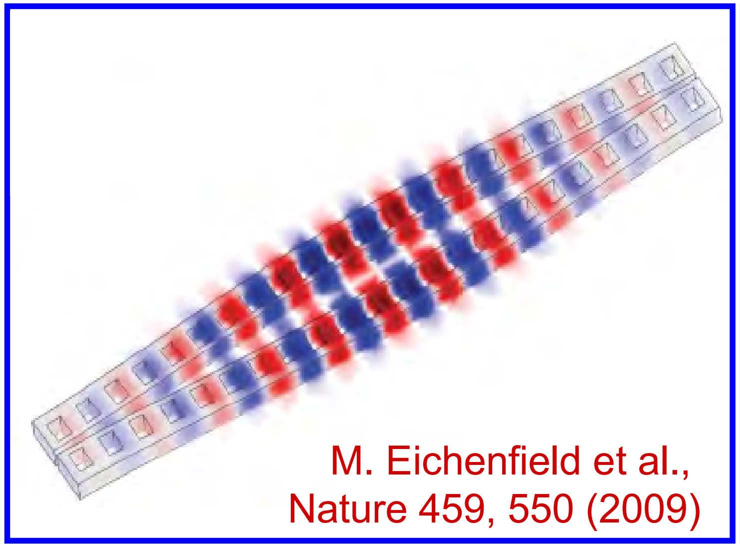

M. Eichenfield et al., Nature 459, 550 (2009)

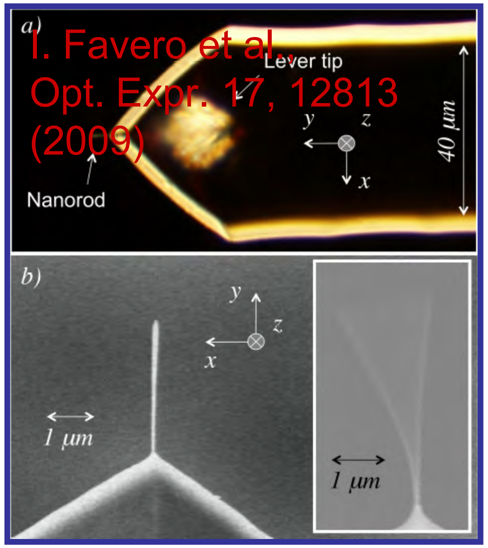

I. Favero et al., Opt. Expr. 17, 12813 (2009)

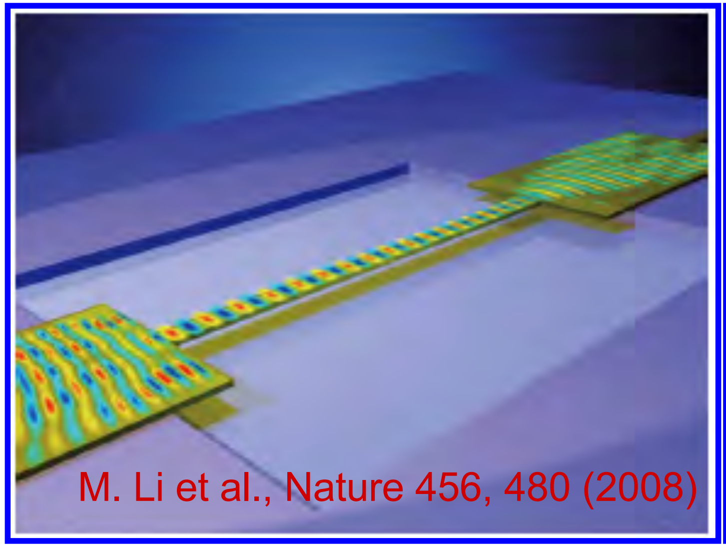

M. Li et al., Nature 456, 480 (2008)

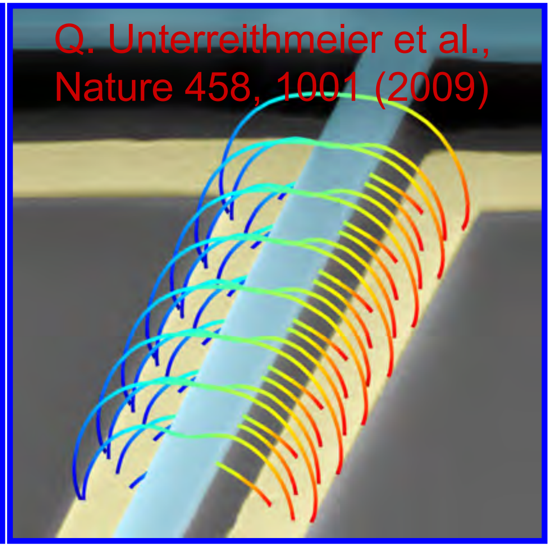

Q. Unterreithmeier et al., Nature 458, 1001 (2009)

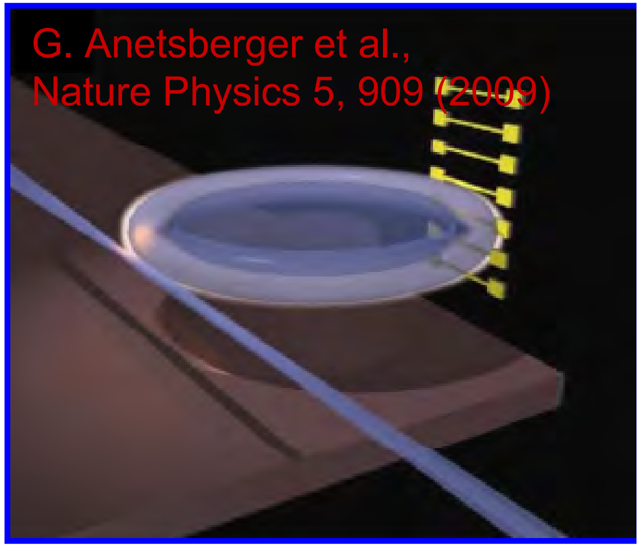

G. Anetsberger et al., Nature Physics 5, 909 (2009)

Cavity - Nanomechanics via optical gradient forces

A stimulating nim -enabled MPQ-LMU collaboration between

The Kippenberg team: Georg Anetsberger, Oliver Arizet et al.

MPQ

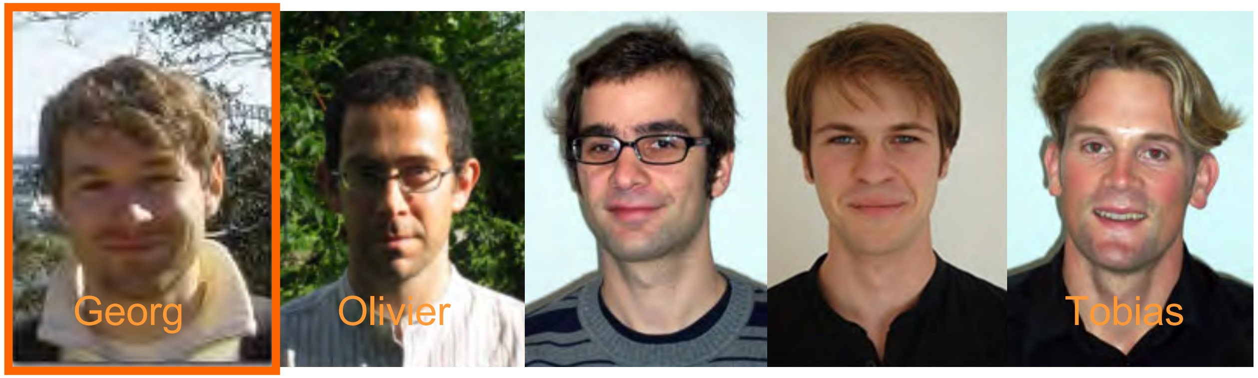

The Kotthaus team: Quirin Unterreithmeier, Eva Weig et al.

LMU LUDWIG-MAXIMILIANS-UNIVERSITÄT MÜNCHEN

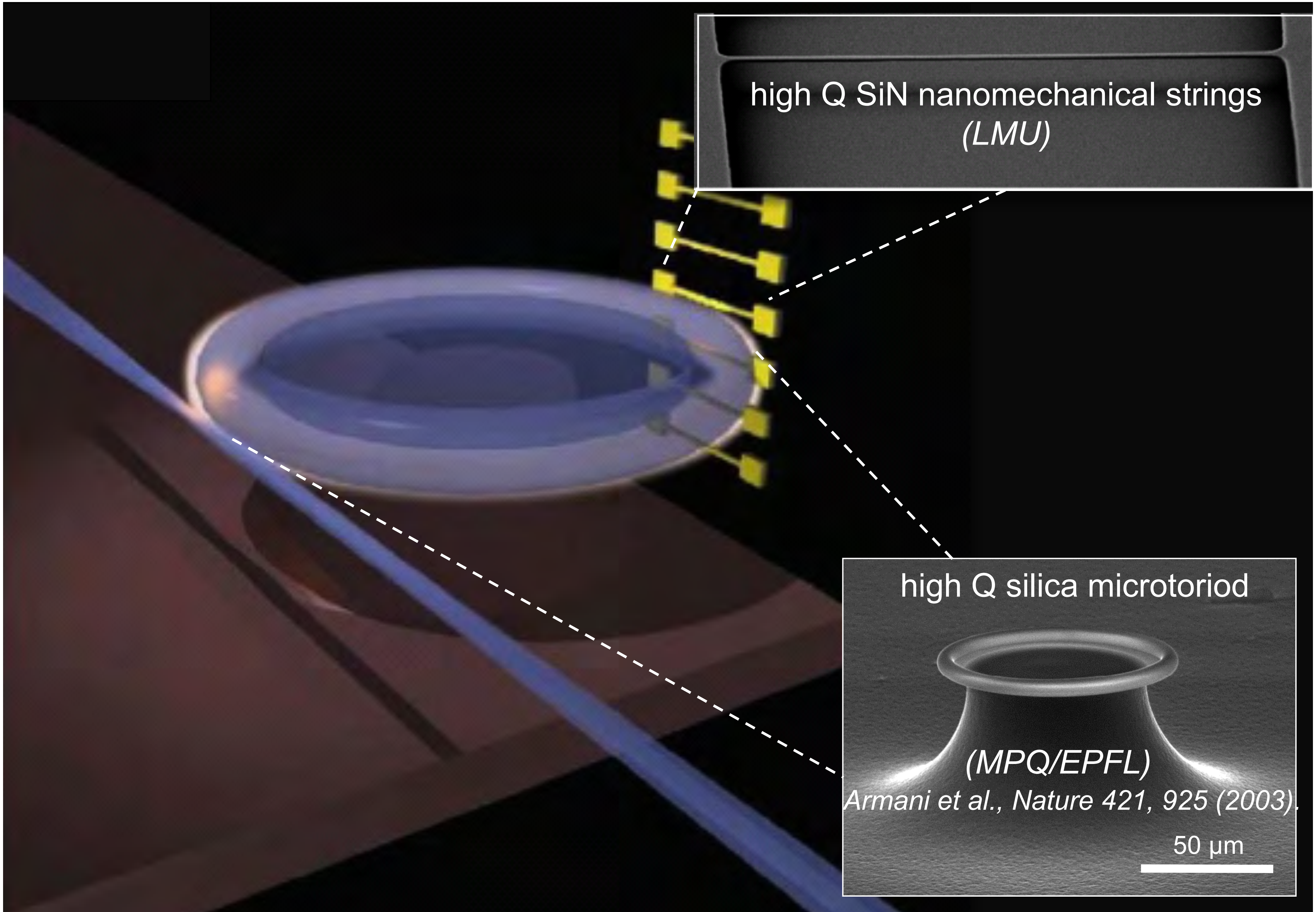

G. Anetsberger, O. Arcizet, Q. P. Unterreithmeier, A. Schliesser, R. Riviere, E. M. Weig, J. P. Kotthaus, T. J. Kippenberg, Nature Physics **5**, 909 (2009)

Concept

Achieve sub-wavelength resolution using optical near-fields

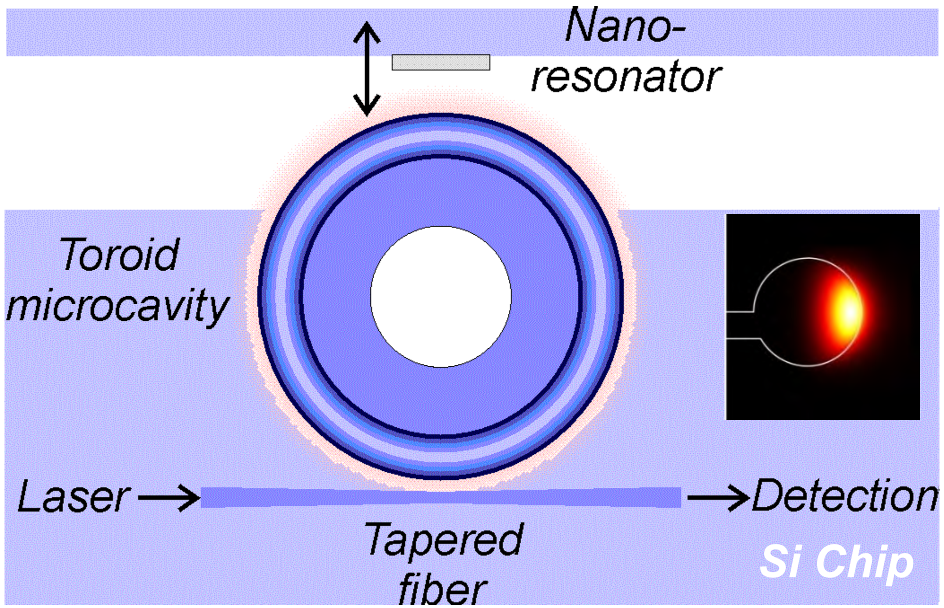

Challenges:

Microfabrication:
- „edge cavities“

Positioning:
- alignment of nanoresonator chip parallel to chip <0.5°
- nanopositioning of fiber *and* resonator
- optical imaging

Absorption?

Fabrication of high Q optical and mechanical resonators

Independent fabrication of cavity and resonator on two separate chips

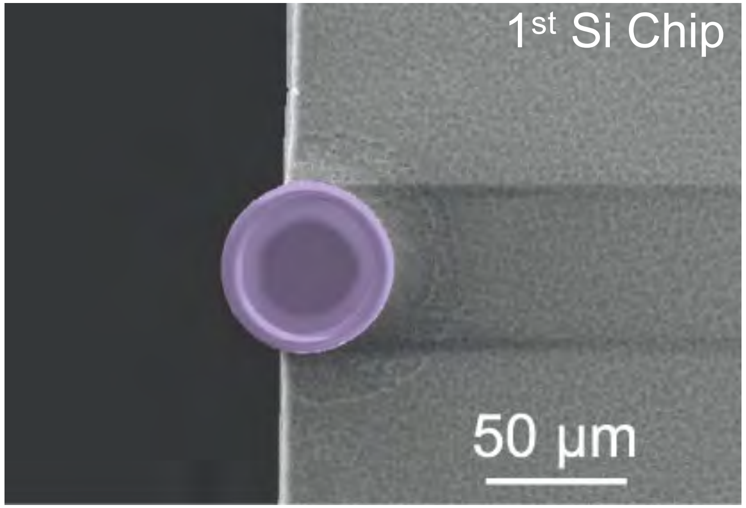

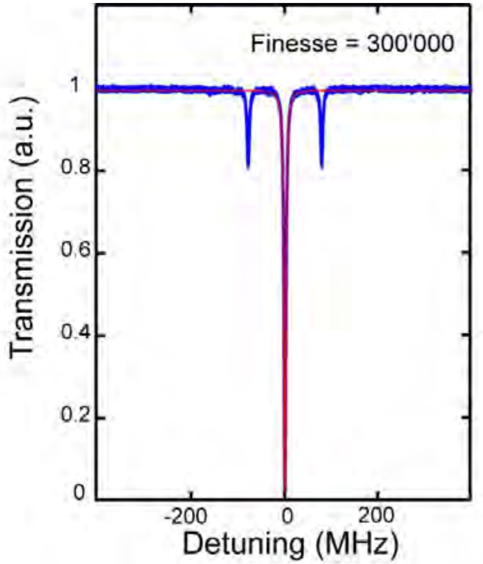

Silica microtoroid

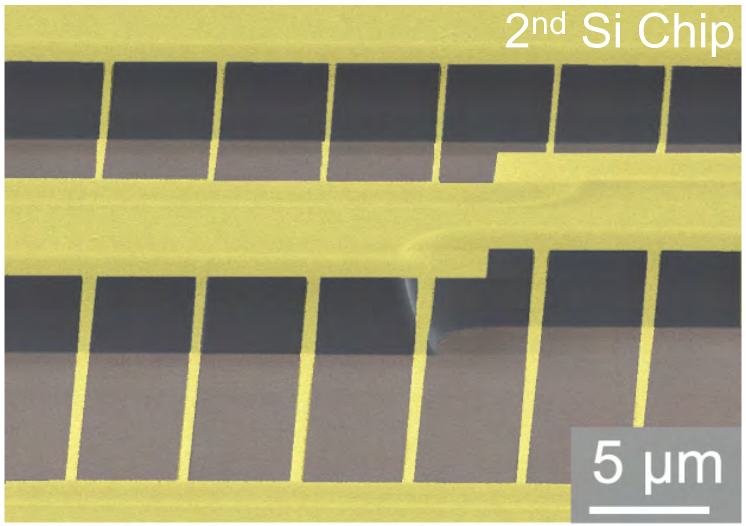

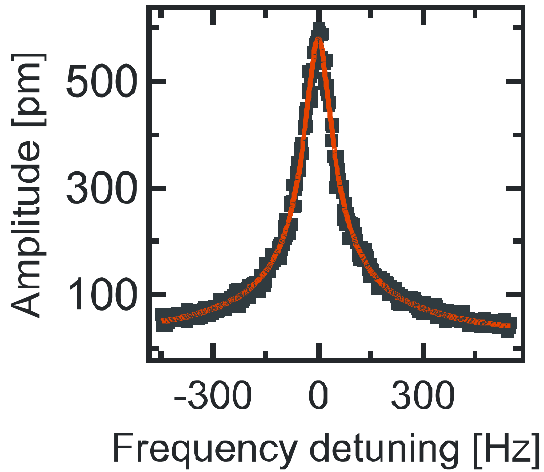

Strained SiN strings

typ. 100nm×500nm×30µm

$\Omega_m/2\pi$=5-15 MHz

$Q_m=10^4-10^5$

m_{eff}=0.9-5 pg

Static optomechanical coupling vs. distance

Interaction with the resonator induces a static shift in cavity frequency

Approaching the resonator in the toroid plane

Cavity frequency shift

$\delta\omega \propto \exp -x/x_0$

$$\delta\omega = \underbrace{\left.\frac{d\omega}{dx}\right|_{x_0}}_{g(x_0)} \delta x$$

static coupling rate:

$$g(x_0) = \left.\frac{d\omega}{dx}\right|_{x_0}$$

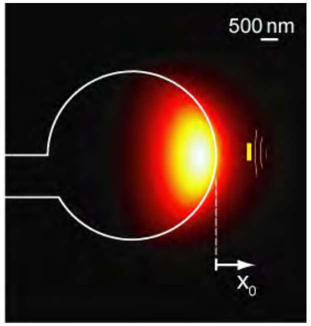

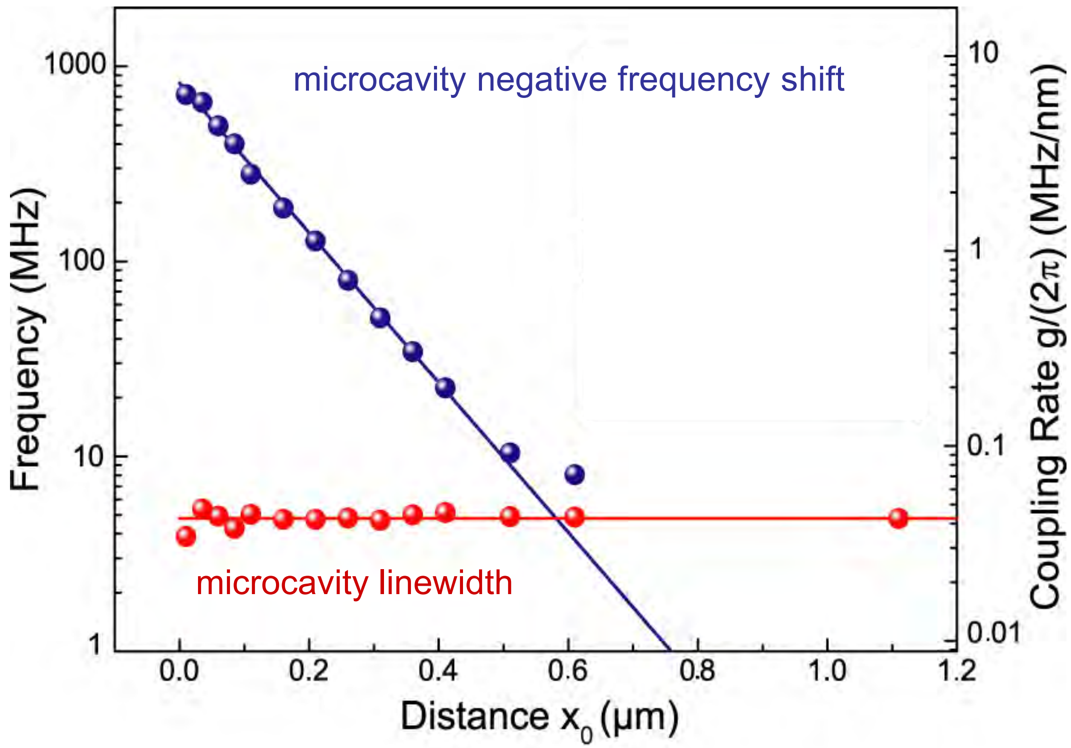

- ⇨ purely dispersive coupling
- ⇨ optomechanical coupling rate $g/(2\pi)$ up to 10 MHz/nm

frequency shifts up to 1 GHz obtained without degrading optical finesse

Dynamic optomechanical coupling

Transduction of Brownian motion of the resonator into cavity frequency noise

Brownian motion imprinted on cavity resonance frequency:

$$\delta\omega = \underbrace{\left.\frac{d\omega}{dx}\right|_{x_0}}_{g(x_0)} \delta x$$

Dynamic measurement of coupling rate:

$$g(x_0) = \sqrt{\frac{S_{\omega\omega}}{S_{xx}}}$$

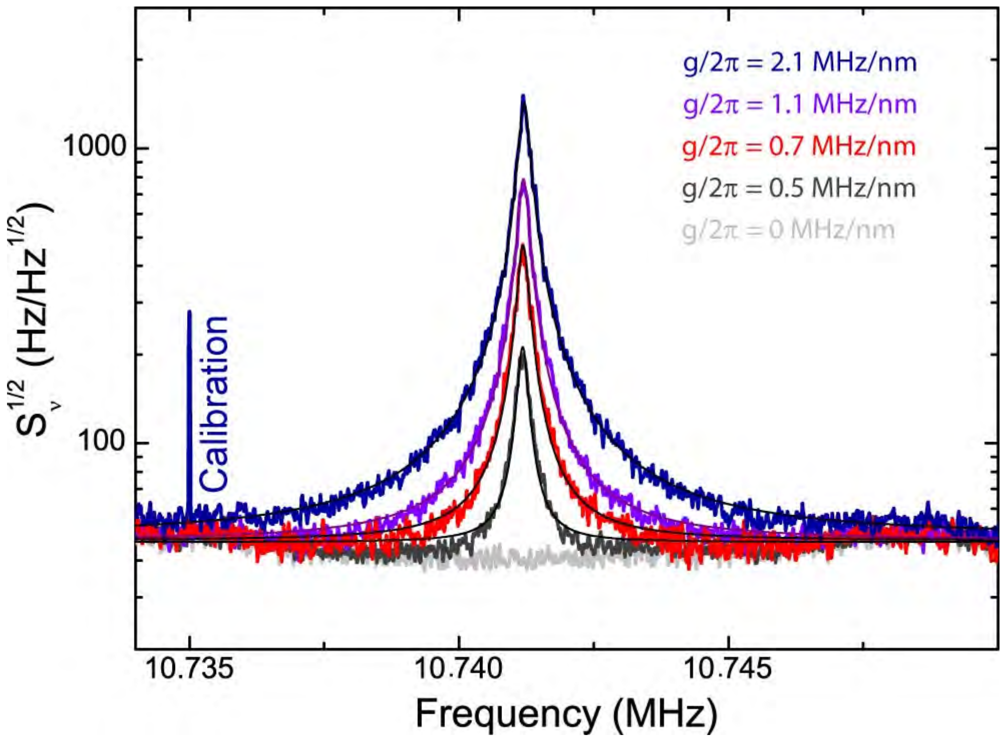

⇨ good agreement with statically determined values

⇨ dispersive coupling with optomechanical coupling rate g/(2π) up to 10 MHz/nm

Quantum limited displacement sensitivity

with sub-femtometer resolution of a nanomechanical resonator at room temperature

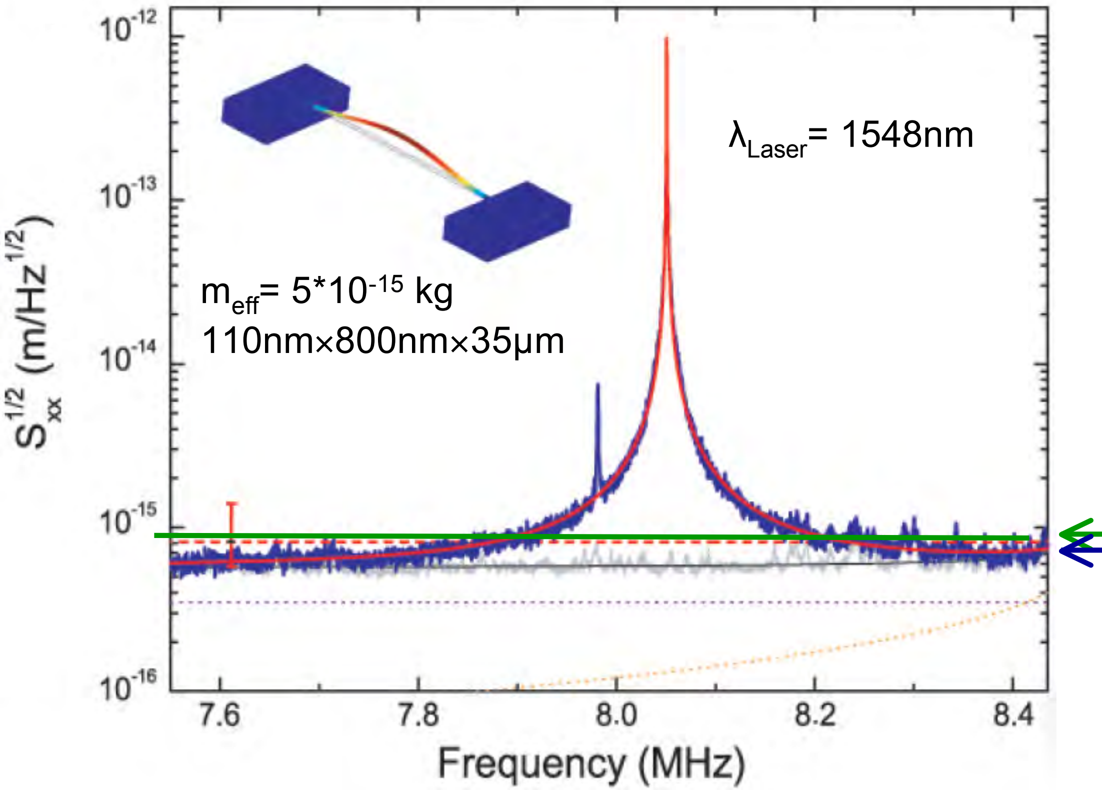

$$\left\langle x(t)^2 \right\rangle_{SQL} = \frac{\hbar}{2m\Omega_m}$$

$$\sqrt{S_{xx}^{SQL}} = \frac{2\hbar Q}{m\Omega_m^2}$$

Standard quantum limit:
$\sqrt{S_{xx}^{SQL}}$ = 820 am/Hz$^{1/2}$

Displacement imprecision:
$\sqrt{S_{xx}^{exp}}$ = 570 am/Hz$^{1/2}$ at 65µW

Laser shot noise:
$\sqrt{S_{xx}^{shot}}$ = 350 am/Hz$^{1/2}$

⇨ state of the art in nanomechanical displacement sensing:

room temperature:	300 fm/Hz$^{1/2}$	interferometric	[*N. O. Azak et al., APL 91, 093112 (2007)*]
	50 am/Hz$^{1/2}$	photonic crystal	[*M.Eichenfield et al., Nature 459, 550 (2009)*]
quantum limited:	5 fm/Hz$^{1/2}$	supercond. circuit	[*J.D.Teufel et al., Nat. Nanotech.4, 820 (2009)*]

Dynamical back action on nanomechanical resonators

via the radiation-pressure-induced optical dipole force

Blue detuned laser

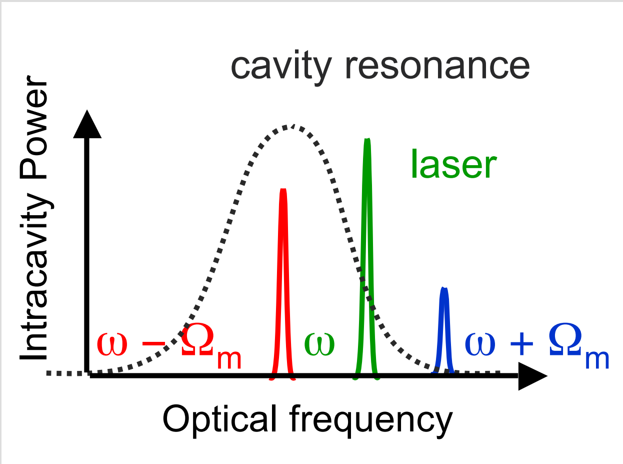

- Stokes processes dominate, net energy transfer from cavity to resonator
- Optomechanical driving

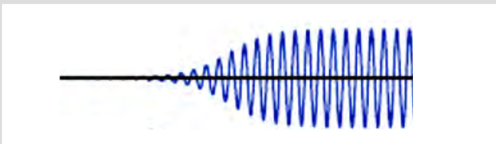

Resolved sideband regime:

$\Omega_m \gtrsim \kappa$

Red detuned laser

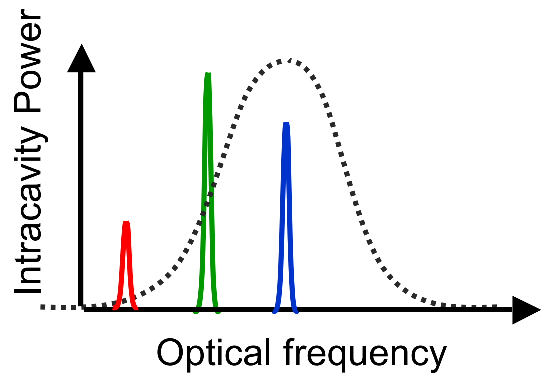

- Anti-Stokes processes dominate, net energy transfer from resonator to cavity
- Optomechanical cooling

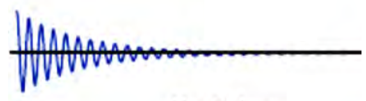

Dynamical back action on the nanomechanical resonator

Radiation-pressure-induced coherent self-oscillation

⇨ Linewidth narrowing:

- Net energy increase corresponds to reduced damping

$$\Gamma = \Gamma_m + \Gamma_{ba} \quad \text{with} \quad \Gamma_{ba} \propto -g^2 \cdot P_{in}$$

⇨ Oscillation threshold and saturation:

- Zero damping at threshold

⇨ Coherent oscillation:

- Radiation pressure induced self-oscillation

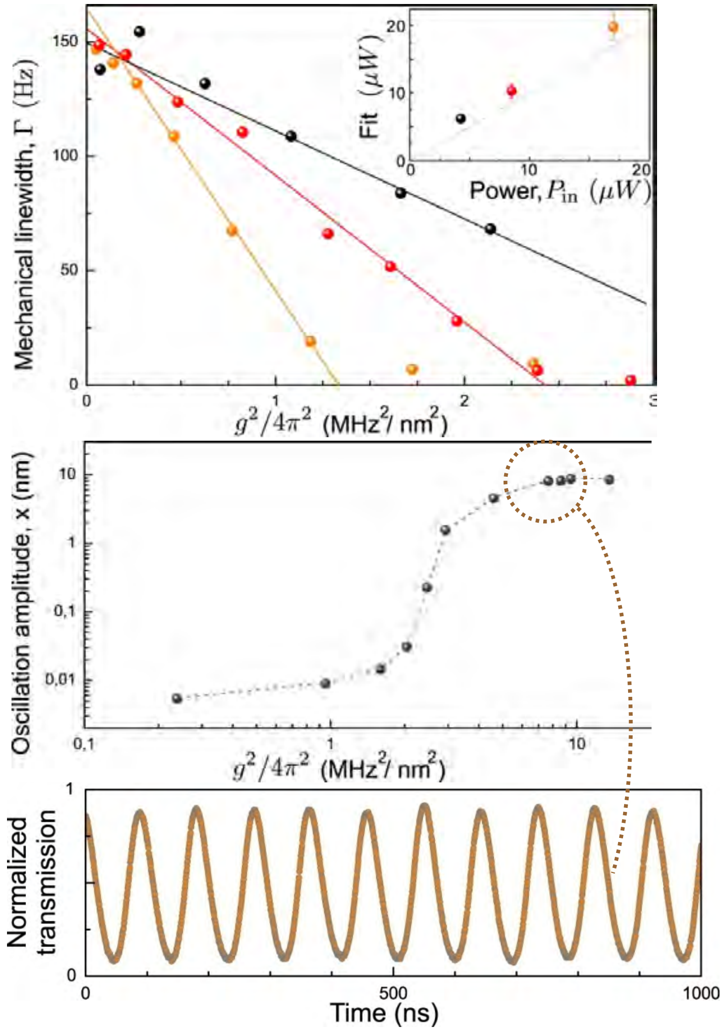

Quantum limits for continuous position measurement

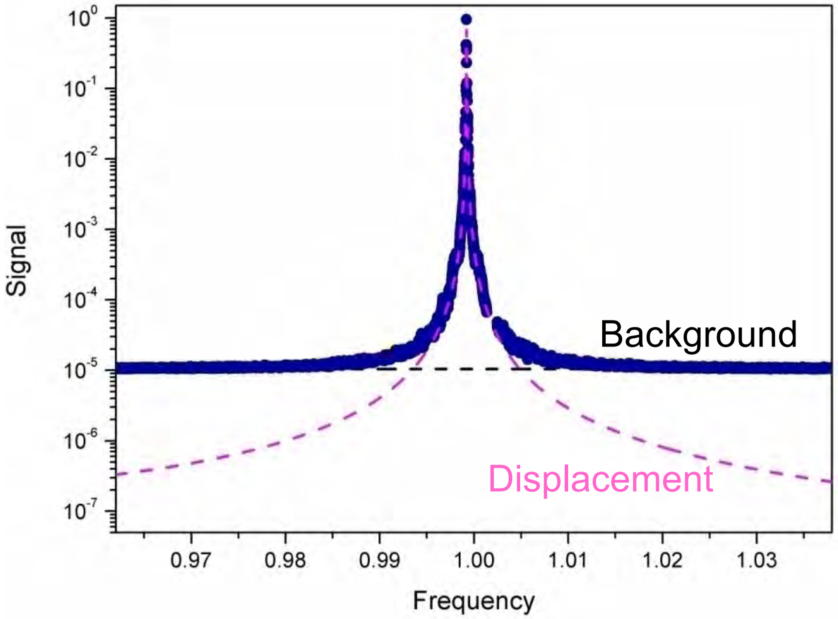

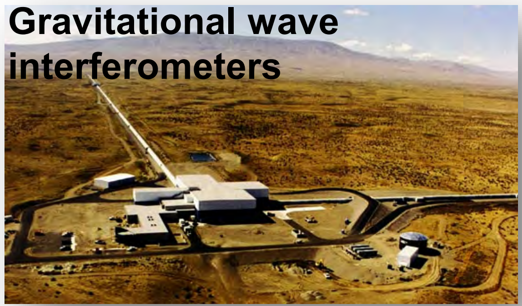

Caves, Phys.Rev. D, 23, 1693 (1981).
Tittonen et al. PRA, 59, 1038 (1999).

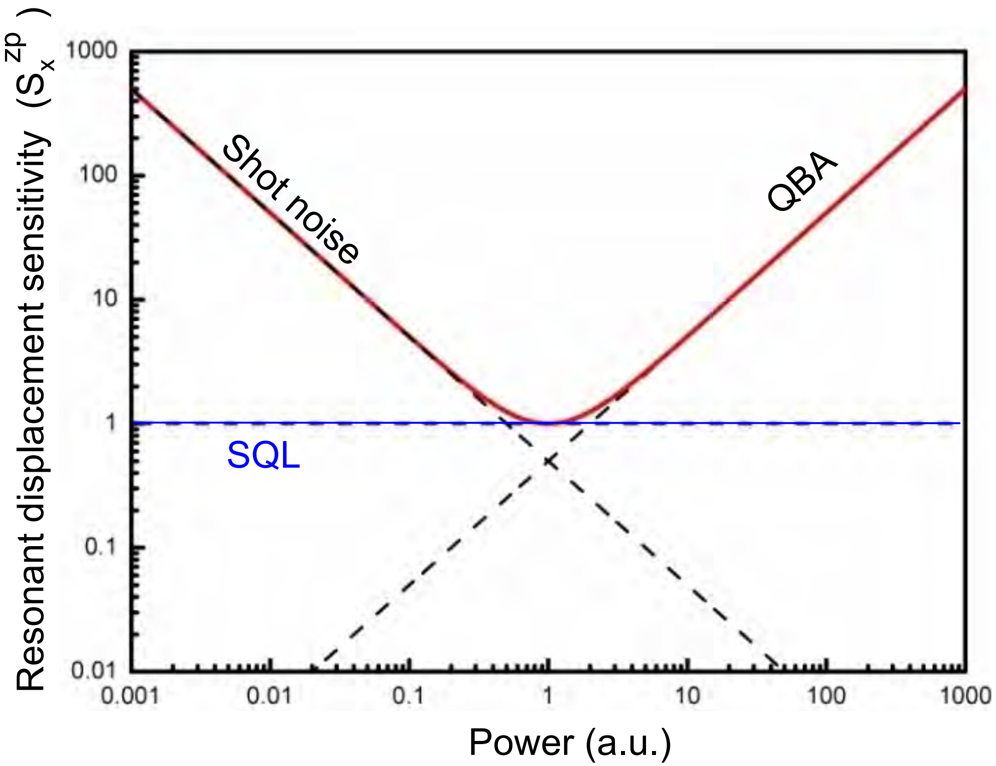

- So far only transducers based on optical cavities are close to shot-noise limit
- Not directly applicable to nanomechanical oscillators due to diffraction

Recent transducers sensitivities for nanomechanical motion

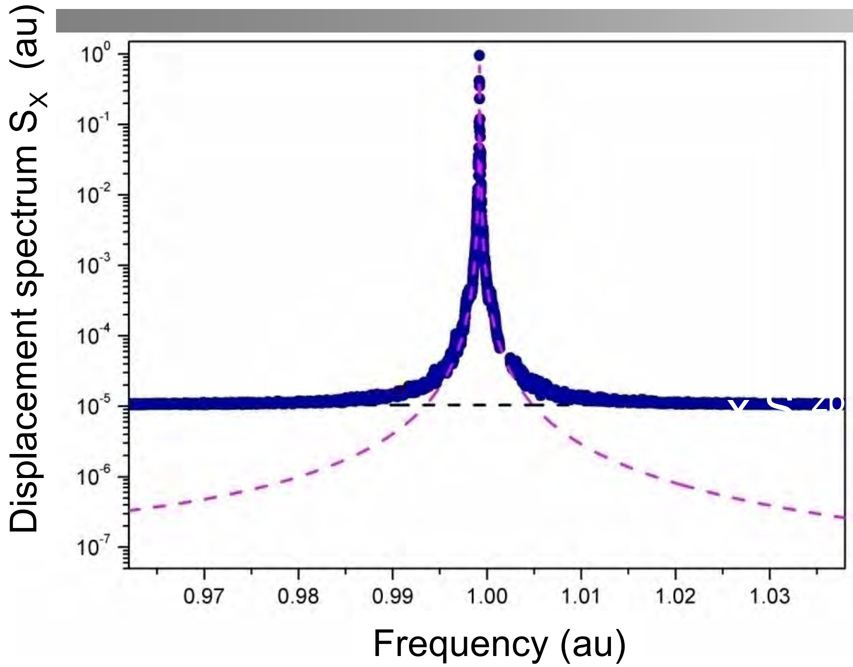

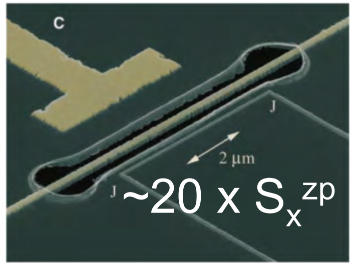

SET

M. D. LaHaye et al., Science, **304**, 74 (2004)

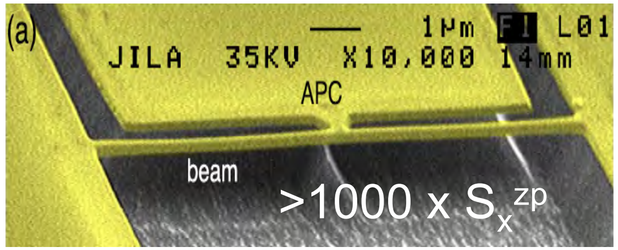

APC

N. E. Flowers-Jacobs, PRL **98**, 096804 (2007)

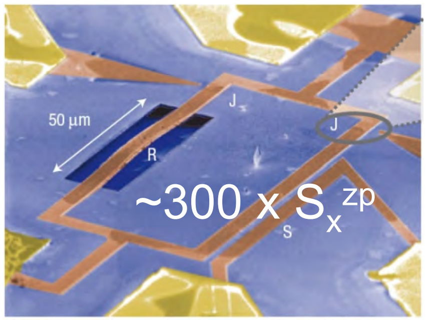

SQUID

S. Etaki et al., Nature Physics **4**, 785 (2008)

Microwave cavity

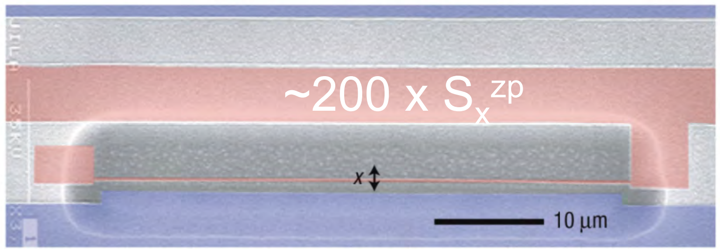

C. A. Regal et al., Nature Physics, **4**, 555 (2008)

Imprecision larger than zero-point motion

Imprecision below the SQL

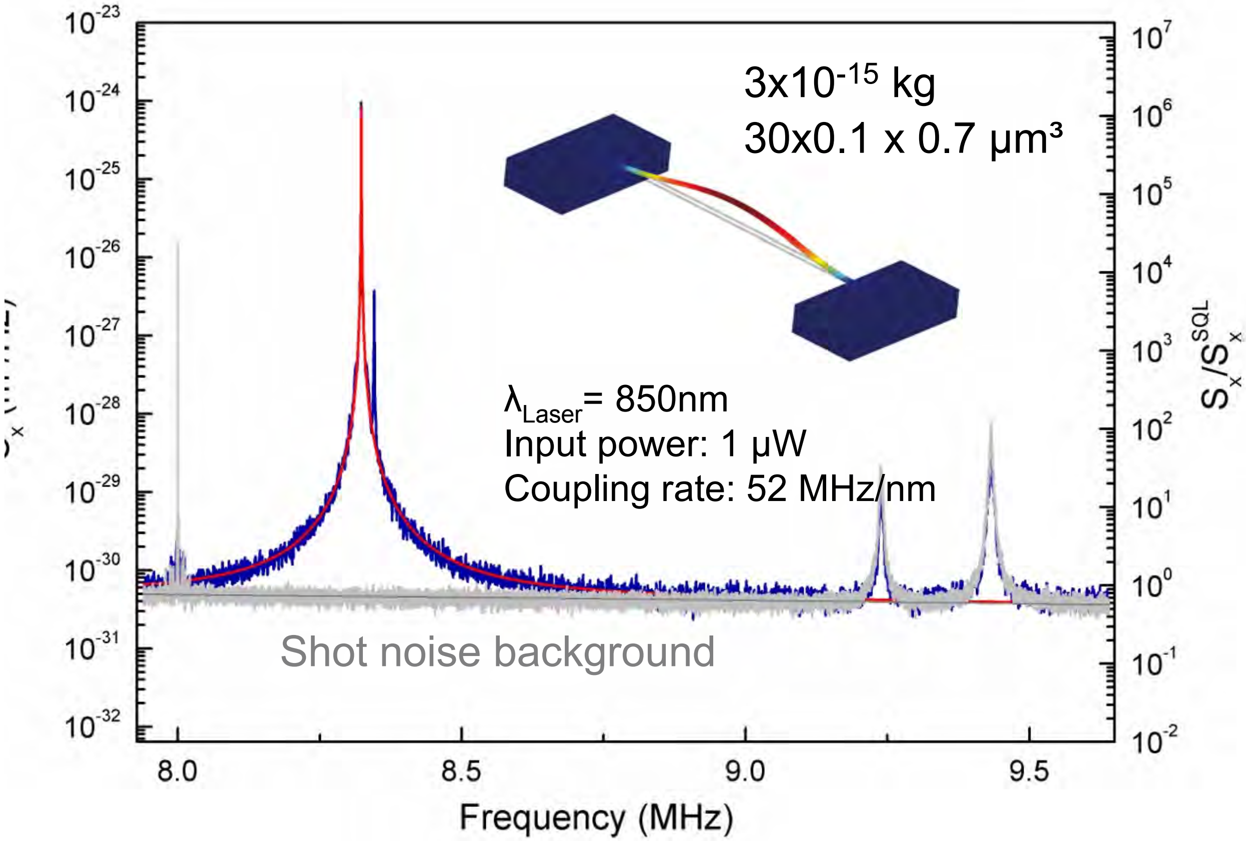

Shot noise limited imprecision:

(600 am/√Hz)2

0.5 x SQL

300 K optical measurement of displacement with an imprecision of 0.5xSQL, expected to go below 0.1xSQL at T< 30K, as limited by thermorefractive noise at 300 K

G. Anetsberger et al., submitted

Optically achieved 300 K-value comparable to imprecision of 0.4´SQL recently measured with microwave cavity at 120m mK

Opens route to explore quantum back-action and back-action evading techniques

J. D. Teufel et al., Nature Nanotechnology 4, 820 (2009)

Nanomechanical charge transport

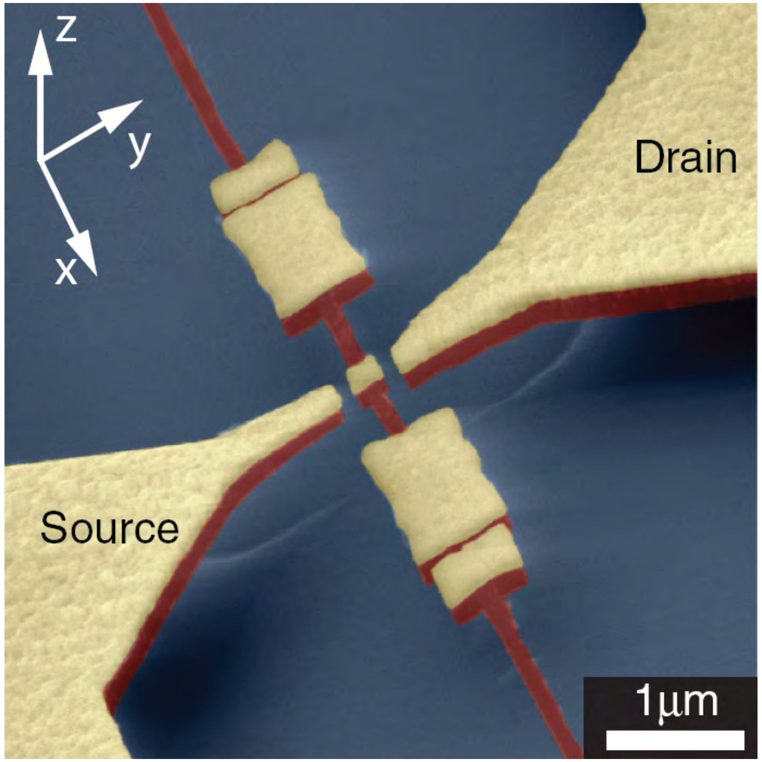

in collaboration with

Daniel König and Eva Maria Weig

A Nanomechanical charge shuttle

The concept of nanomechanical (single) electron transport

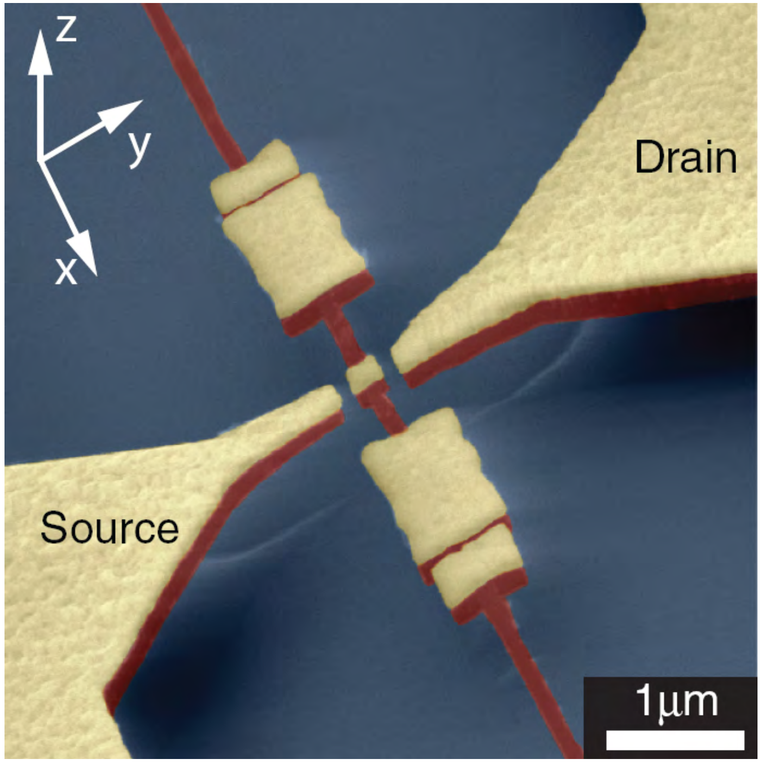

Mechanical actuation of an electrical current:

$$\bar{I}_{sd} = 2 \cdot \bar{n} \cdot e \cdot f$$

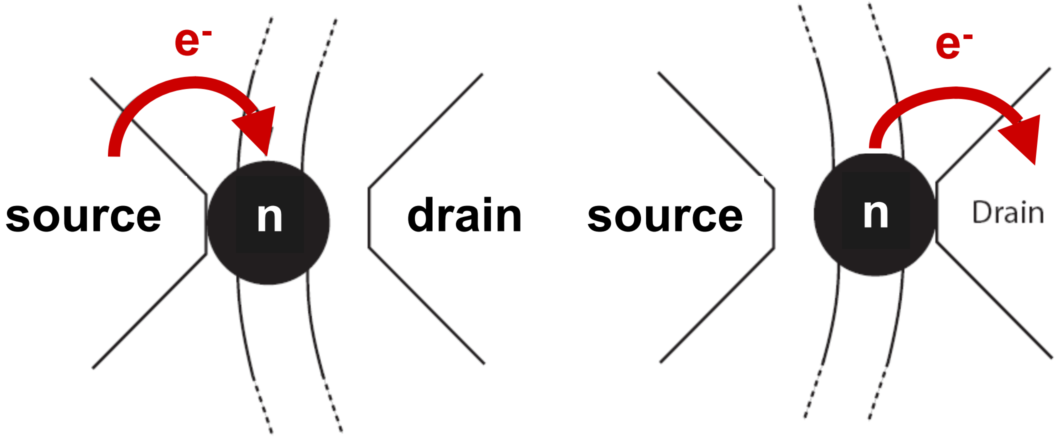

as theoretically proposed by

L. Y. Gorelik et al., PRL 80, 4526 (1998)

A short history of shuttles

The quest of finding the right actuation mechanism to enter the Coulomb blockade regime

ac drive via auxilliary gates:

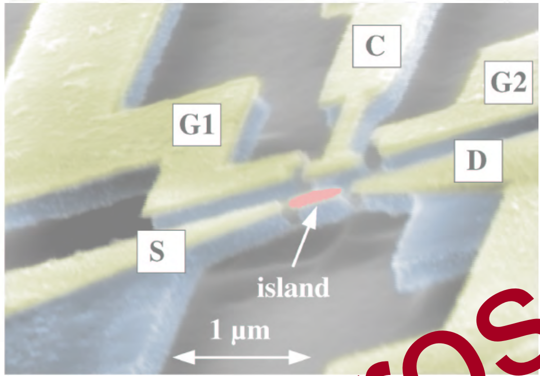

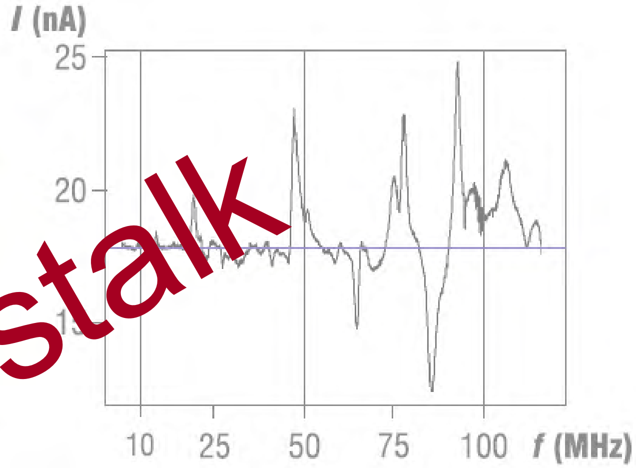

A. Erbe et al., Phys. Rev. Lett. 89, 096106 (2001)

or: D. Scheible et al., NJP 12, 023019 (2010)

electrical crosstalk

direct ac drive:

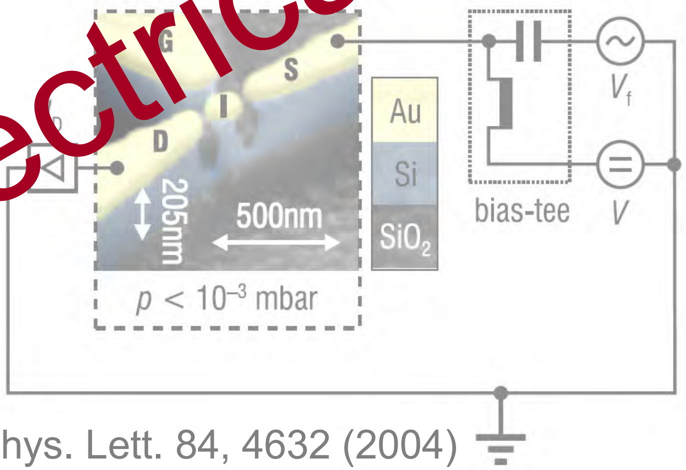

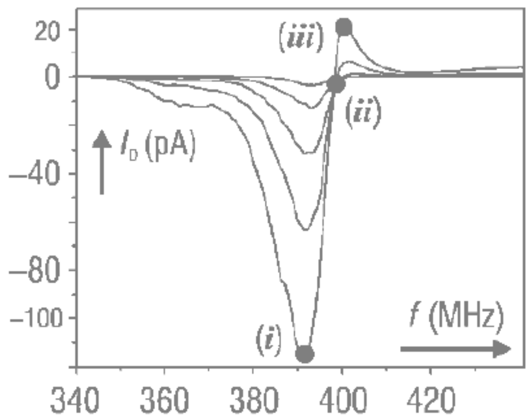

D. Scheible et al., Appl. Phys. Lett. 84, 4632 (2004)

Inertial actuation of the shuttle

using acoustic waves produced by a piezo transducer shielded by a Faraday cage

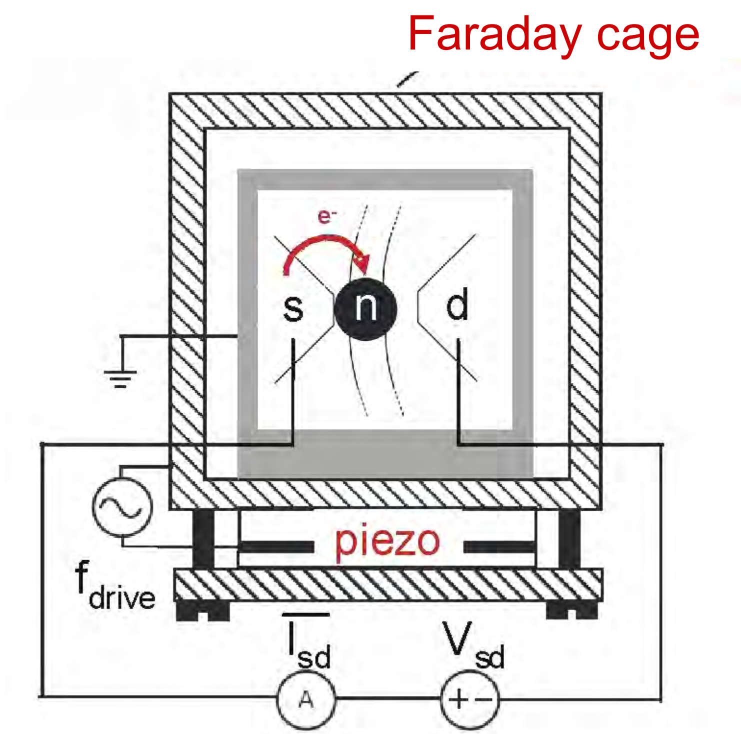

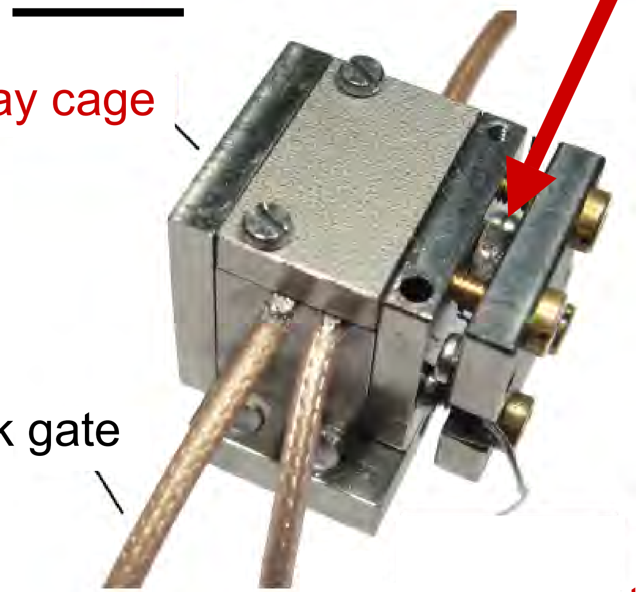

measure time-averaged source-drain current across the island

Faraday cage ensures complete decoupling from the drive signal

König, Weig, Kotthaus, Nature Nanotechnology 3, 482 (2008)

Transport characterization of individual shuttles

Not all shuttles display stable mechanical trajectories giving rise to charge transport

Piezo-driven electron shuttling at T = 20 K:

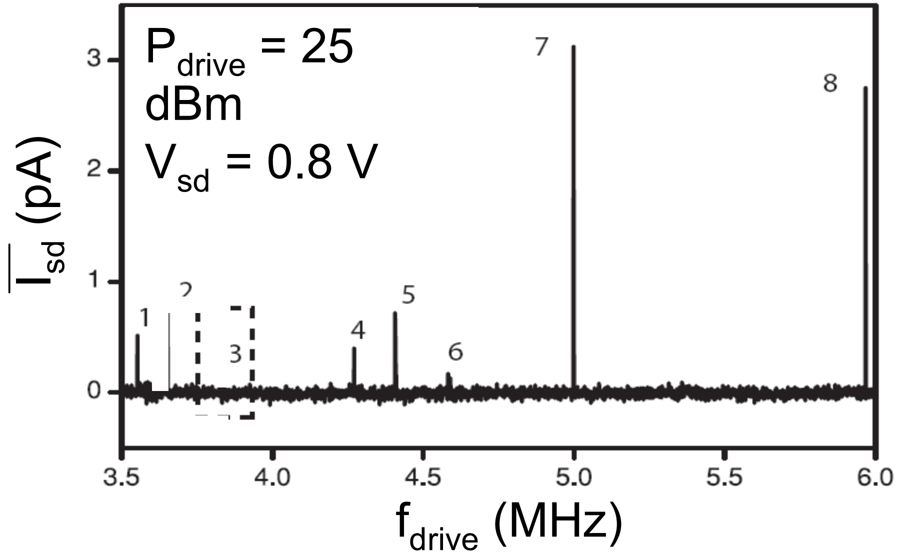

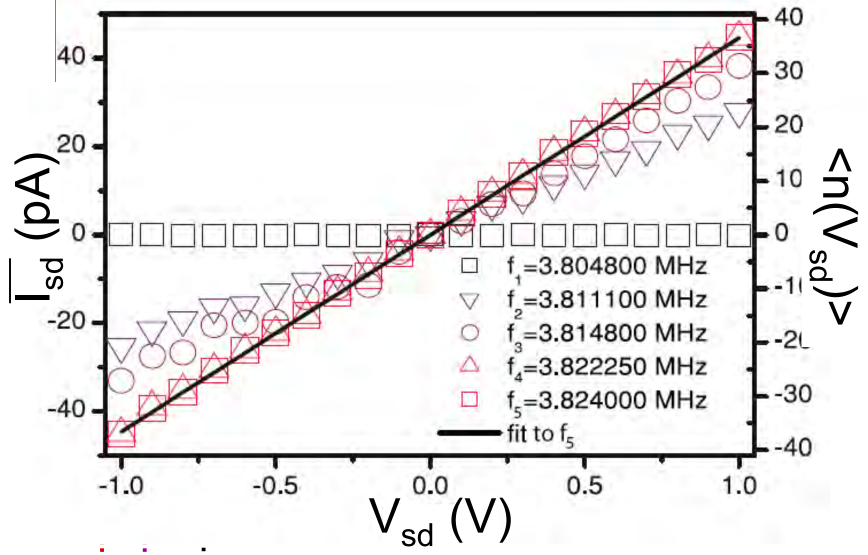

no transport (off-resonant)

subharmonic / irregular dynamics:
transport mechanically limited

2π-periodic dynamics:
transport capacitively limited

model: single electron box

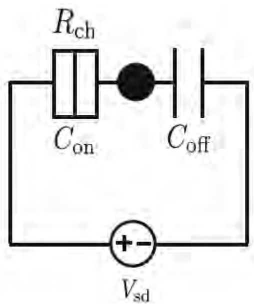

high-temperature regime

⇨ C_{off} = 5.94 aF

A mechanical *single* electron shuttle?

Prerequisites for entering the Coulomb blockade regime

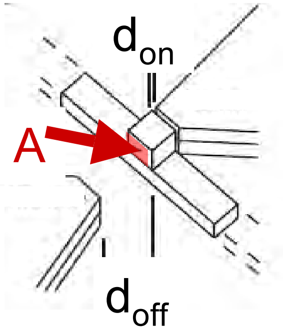

island cross section area
A = 140 nm x 60 nm

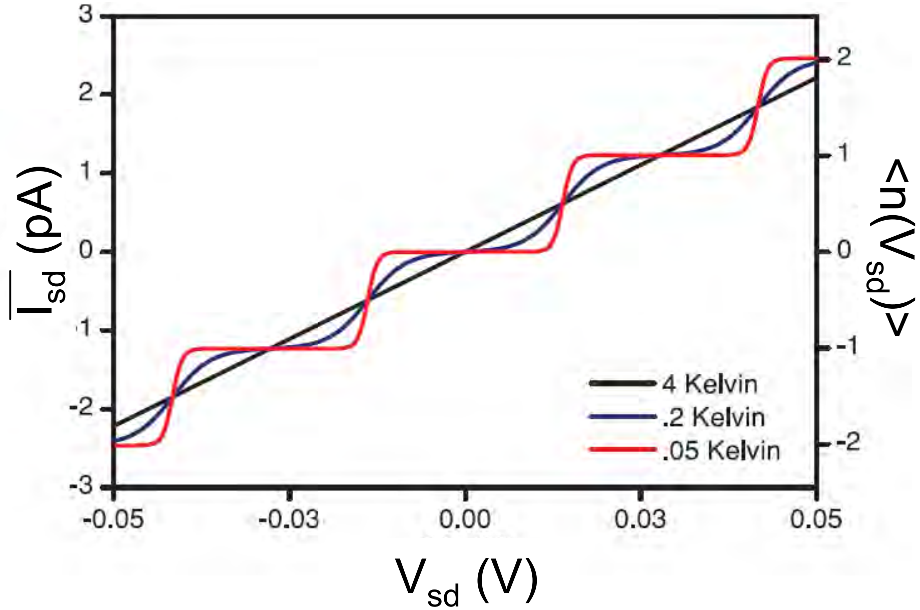

Coulomb blockade at 200 mK

"Coulomb blockade"

fixed electron number on the island: thermal energy must not exceed the charging energy

$k_B T \ll e^2/2C_\Sigma$

lower temperatures

non-dissipative actuation scheme

larger charging energy

smaller island

Nanomechanical charge shuttle

The concept of nanomechanical (single) electron transport

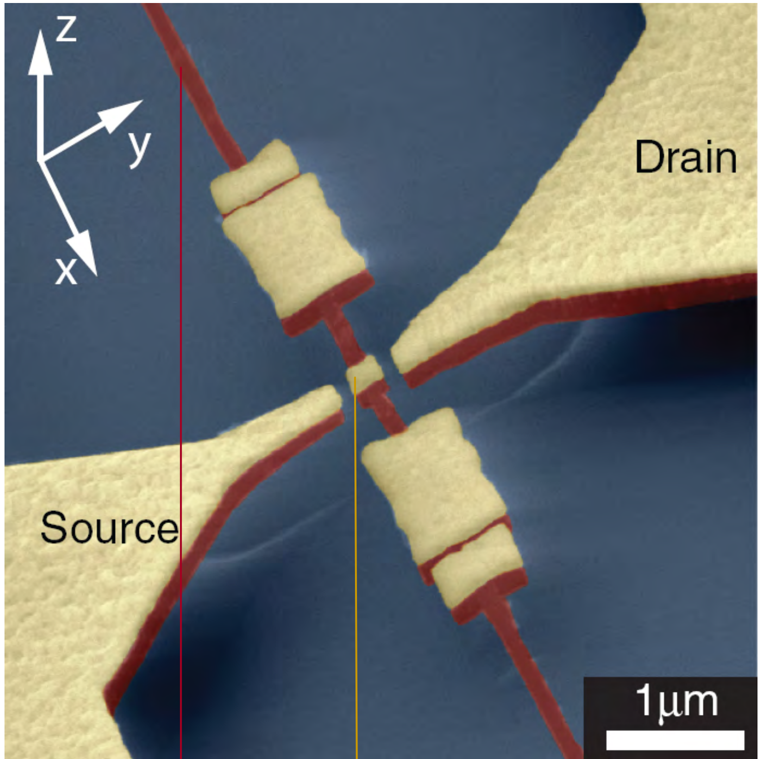

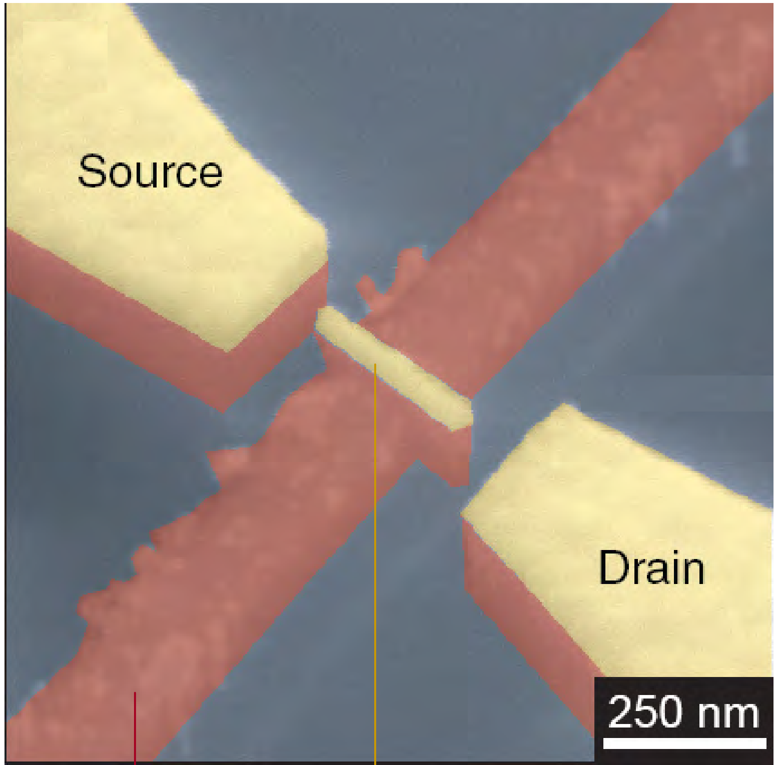

island:
170 nm x 140 nm x 60 nm

resonator:
14 µm x 70 nm x 110 nm

island:
270 nm x 30 nm x 20 nm ÷ 250

resonator:
14 µm x 130 nm x 110 nm vs.

Voltage-induced self-oscillation

Self-sustained shuttling for bias voltage exceeding shuttle dissipation threshold

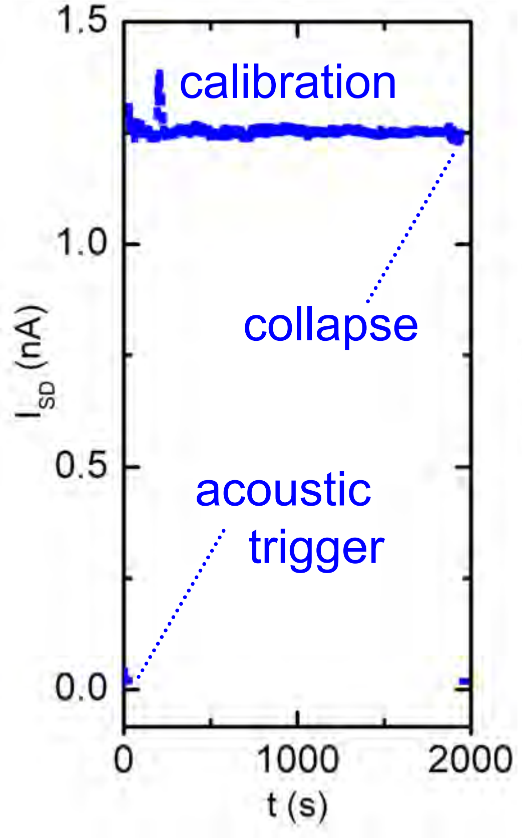

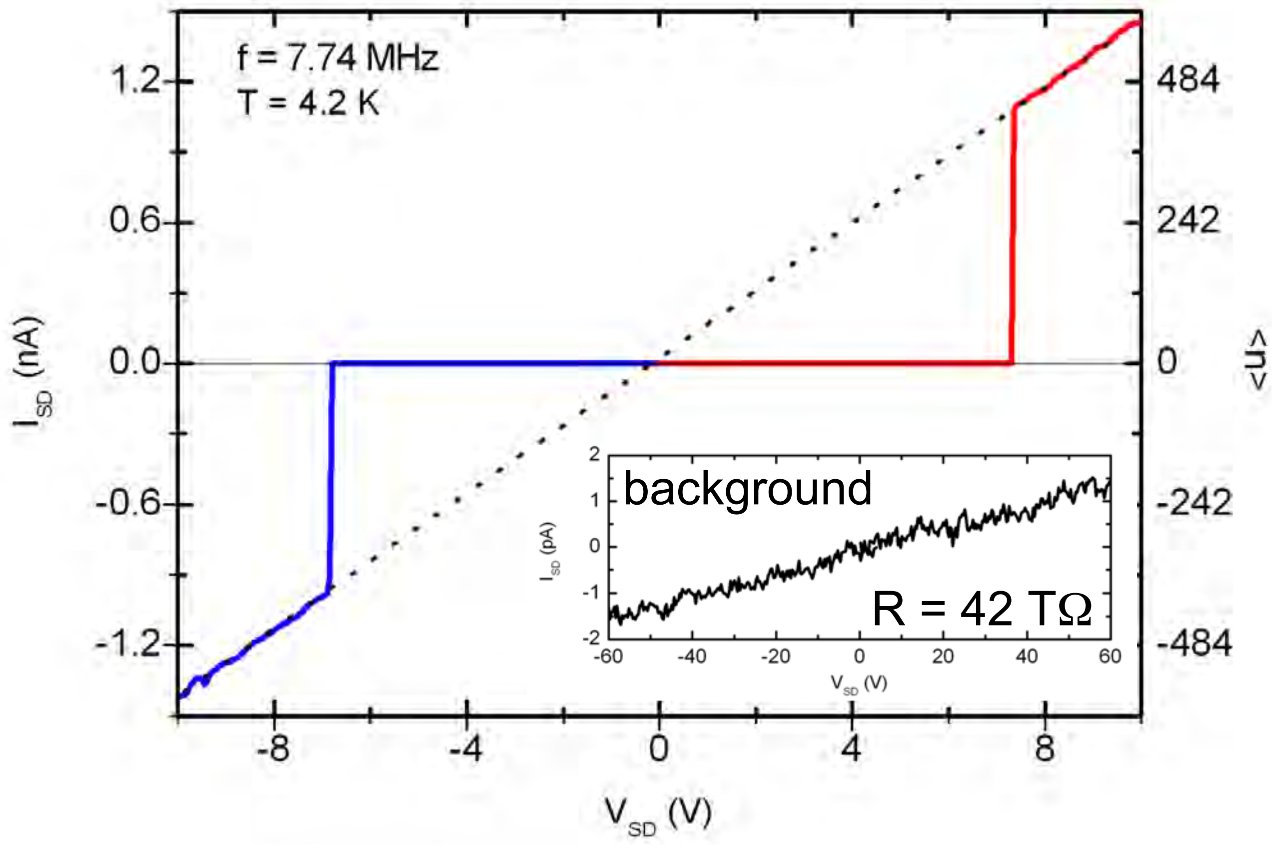

V_{SD} = 12 V

- mechanically dissipated energy P_{diss} = 2-8 nW
- no field emission up to V_{DC} = 60 V
- operation at 4.2 K

SUMMARY

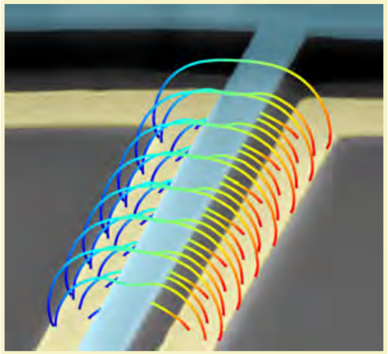

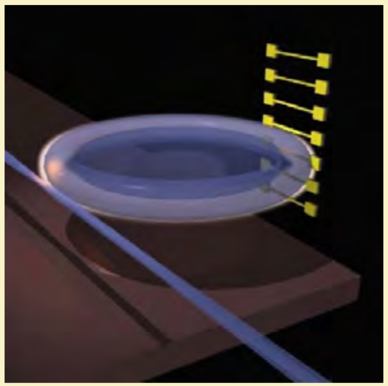

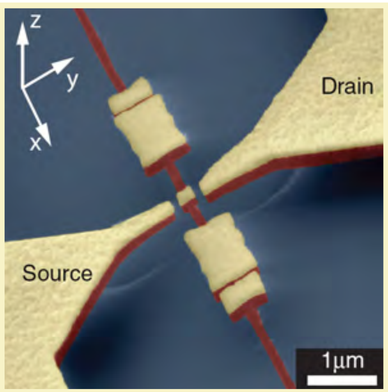

Transduction via dielectric gradient fields

- External yet local actuation of dielectric resonators
- Integrated optoelectronic detection
- Control of linear and non-linear dynamics
- High Q in stressed resonators understood
- Progress towards an understanding of damping
- On route to scalable and efficient on-chip NEMS

Near-field cavity nano-optomechanics

- Platform extending dispersive cavity optomechanics to the nanoscale
- Dynamical back action on nanomechanical oscillators
- Imprecision of motion detection at 300K below SQL

Nanomechanical charge shuttle

- Capacitance controlled electron shuttling demonstrated
- Self-oscillation observed
- Approaching Coulomb blockade regime

Thank you, for your attention!